Metal Particle Detection Methods and Their Use for Freeze-Dried Vaccine Inspection: A Review

Jack B. Jedlicki, Denise Tellbach, and Brian Subirana

***Abstract*—We establish a set of metal particle detection methods that are suitable for automated inspection of freeze-dried vaccines. We first identify the requirements for freeze-dried vaccine inspection. We then assess metal particle detection methods obtained through a comprehensive literature review with the requirements for automated inspection. In particular, we find inductive sensors, superconducting quantum interference device (SQUID)-based sensors, giant magnetoresistive (GMR)/tunneling magnetoresistive (TMR)-based sensors, and THz imaging, hyperspectral imaging, thermal imaging, X-ray inspection, and radio frequency identification (RFID)-based sensors promising for automated inspection of freeze-dried vaccines. However, experiments assessing the applicability of these methods for freeze-dried vaccine inspection are severely limited, and future research is required to choose the best performing methods.**

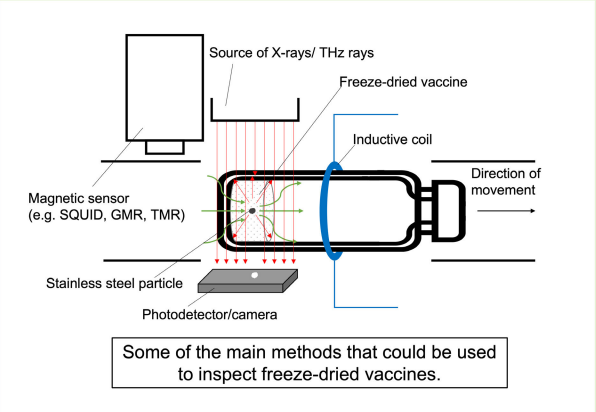

Some of the main methods that could be used to inspect freeze-dried vaccines.

***Index Terms*— Automated control, conductive particles, lyophilized vaccines, quality monitoring, turbid, visually opaque media.**

I. Introduction

EFFECTIVE quality control is a common challenge for two major developments to meet global vaccine demand: 1) increasing production capacity through continuous manufacturing and 2) creating thermally stable vaccines through freeze drying [1].

The production volume of vaccines is steadily increasing to meet demand; for example, the global production capacity for pandemic vaccines rose from 6.2 billion (2013) to more than 12 billion doses (2021) annually [2], [3], [4]. However, expanding production capacity requires real-time quality control and introduces new modes of failure [5], [6].

Freeze drying solves several issues of thermally unstable vaccines [7], [8], [9], such as eliminating stringent cooling requirements [10], which can account for up to 80% of vaccination cost [11], and improving accessibility to vaccines. For example, COVID-19 vaccines require storage and transportation temperatures between −80 °C and −20 °C for a lifetime of three to six months with stable lifetime dropping to only 2–24 h at room temperature [12], [13]. Approximately two-thirds of the world population live in a country without the necessary refrigeration technology available to ensure an unbroken cold chain [14], leaving an estimated three billion people without access to COVID-19 vaccines due to a lack of cold storage [15]. However, freeze drying of vaccines makes a visual inspection of final products more difficult due to the visually opaque nature of freeze-dried vaccines, which can fully or partially obscure defects such as metal particles [16] and the resemblance between defects and normal product appearance variation [17].

One particular issue for quality inspection of vaccines is the elimination of metal particles in vaccine products before they leave the production facility. Metal particles pose a risk to patients in the form of adverse effects on their health [16], [18]. We know that metal particles have led to high-profile recalls of millions of vaccines in the past years. For example, 1.63 million doses of Moderna's COVID-19 vaccine were recalled after distribution to patients had already started in Japan in 2021 [19], [20].

In this work, we examine the literature on existing methods for metal particle detection with regard to their suitability for inspection of freeze-dried vaccines. We first establish the

Manuscript received 30 May 2023; revised 25 July 2023; accepted 25 July 2023. Date of publication 6 November 2023; date of current version 2 January 2024. This work was supported in part by Takeda Development Center Americas, Inc. (successor in interest to Millennium Pharmaceuticals, Inc.). The associate editor coordinating the review of this article and approving it for publication was Dr. Richard T. Kouzes. *(Corresponding author: Brian Subirana.)*

Jack B. Jedlicki is with the Department of Mathematics and Computer Science, University of Barcelona, 08007 Barcelona, Spain (e-mail: jbenarje7@alumnes.ub.edu).

Denise Tellbach is with the Auto-ID Labs, Massachusetts Institute of Technology, Cambridge, MA 02139 USA (e-mail: tellbach@mit.edu).

Brian Subirana is with the Massachusetts Institute of Technology, Cambridge, MA 02139 USA, also with Harvard University, Cambridge, MA 02138 USA, and also with the EADA Business School, 08011 Barcelona, Spain (e-mail: subirana@mit.edu).

Digital Object Identifier 10.1109/JSEN.2023.3324278

requirements for the successful inspection of freeze-dried vaccines for metal particles and use these requirements to assess the metal particle detection methods identified in the literature.

The remainder of this article is structured as follows. We discuss related work in Section II. Section III outlines our methodology for literature selection and handling. We discuss the requirements for a promising metal particle detection method for vaccine inspection in Section IV. We then present a summary of metal particle detection methods and discuss them in relation to the requirements of inspection of freeze-dried vaccines in Section V. Next, we discuss the potential fulfillment of vaccine inspection requirements and outline the future work required to meet them in Section VI. Finally, we summarize our findings and outline potential future avenues for research in Section VII.

II. Related Work

A. Inspection of Freeze-Dried Vaccines

Current approaches for inspection of freeze-dried vaccines encompass manual inspection by human operators and semi-automated inspection with automated handling but human inspection and fully automated inspection using line cameras [21]. All commercially rolled-out technologies have in common that they are incapable of detecting any defects under the surface of the freeze-dried vaccine cake.

Research on new inspection methods for vaccines, both liquid and freeze-dried, explores data processing and sensing technology approaches to enhance computer vision [22]. While machine learning (ML)-based methods using line camera input are able to operate inspection at high speed, they lack the ability to identify subsurface features [23], [24], [25], [26]. In contrast, some novel sensing techniques, such as near-infrared (IR) spectroscopy [27] and nuclear magnetic resonance (NMR) relaxometry [28], are capable to discern subsurface vaccine features but lack the ability to detect metal particles. A recent review of nondestructive inspection methods for solid particles in freeze-dried vaccines compares a number of spectroscopy and imaging techniques. While this review assesses the ability of different methods for the detection of metal particles among other types of particles, it fails to present a comprehensive picture of metal particle detection methods [29].

The work specifically on metal particle detection in vaccines is limited, even more so for freeze-dried vaccines. Metal particles, even trace amounts, in vaccines have been detected using atomic absorption spectrometry, atomic emission spectrometry, flame emission spectrometry [30], and energy dispersive X-ray spectroscopy [20]. However, these methods are very slow (on the order of hours) and require the destruction of the investigated vial specimen, therefore being unsuitable for automated inspection of 100% of vaccine vials.

B. Current Reviews of Metal Particle Detection

Multiple previous works provide reviews of methods for metal particle detection. However, each of these reviews leaves gaps that we are seeking to close in this work. Previous reviews can be grouped according to their area of focus. One group of reviews discusses metal particle detection methods related to a specific area of application, and the second group discusses methods belonging to a specific type of metal particle detection method or methods focused on detecting a certain type of metal particle.

Reviews of metal particle detection methods presented in [31], [32], [33], [34], [35], [36], and [37] focus solely on methods that apply to wear monitoring in lubricant oil by detecting metal particles of sizes between approximately 1 μm and 1 mm. [31], [32], [33], [34]; all mainly focus on online detection methods, such as photodetector, resistive–capacitive sensor, acoustic sensor, and inductive sensor with [31] and [33] classifying the sensors into acoustic, optical, electric, and magnetic sensors. Yang et al. [34] exclusively focus on inductive sensors. Jia et al. [31], Wei et al. [32], Sun et al. [33], Myshkin and Markova [35], and Lukas and Anderson [37] omit online sensors not prevalent in lubricant oil analysis, such as X-ray imaging, THz cameras, thermal cameras, and lensless imaging. Regarding offline detection methods in addition to online detection methods, Wei et al. [32] and Myshkin and Markova [35] provided a surface-level review of methods such as optical microscopes, electron microscopes, and X-ray diffraction (XRD). While Murali et al. [36] include both online and offline methods in the review, the working principles of detection methods are not discussed. Jia et al. [31] and Sun et al. [33] do not include offline detection methods in their review. Lukas and Anderson [37] limit their review to an incomplete summary of the main methods, both online and offline of metal particle detection in lubricant oil, primarily covering spectrometry and ferrography. The aforementioned reviews, therefore, paint an incomplete picture of metal particle detection methods.

Other works review methods for metal particle detection in pure water [38] or aqueous solutions [39]. While Tutulea et al. [39] focus on electrochemical sensors for detecting metal ions, Trumsina et al. [38] discuss detection methods for nanoparticles such as microscopy, spectroscopy, tracking analysis, and electrography.

Davis [40], Rao [41], Hunt [42], Humphrey and Martin [43], and Davies [44] review metal particle detection methods for the purpose of condition monitoring in commercial applications, which means the detection of metal particles in fluids, mainly lubricant oil. However, with the exception of [44] that was published ten years ago, all these reviews are over 20 years old, which means that they do not include recent advances in detection methods, such as superconducting quantum interference device (SQUID) sensors, magnetoresistive sensors, inductive sensors, and other methods.

Other reviews have focused their reviews on specific types of metal particle detection methods. Abedini-Nassab et al. [45] review magnetic sensors with a focus on magnetoresistive sensors, SQUID sensors, and magnetorelaxometry. Xu et al. [46] focus on the detection of heavy metal ions through surface-enhanced Raman scattering.

C. Novelty and Contribution of Our Approach

Based on the aforementioned reviews, the research of metal particle detection is split among different types of applications, and a review covering the entire field of metal

TABLE I
DETAILED SEARCH TERMS AND RESULTS OF METAL PARTICLE DETECTION METHODS IN THE LITERATURE

Step	Search Term	Results Count	Relevant Results
1	"Detection of metal particle"	6	2
1	"Detection of metal particles"	148	77
1	"Metal particle detection"	136	79
1	"Metal particles detection"	32	16
1	"Metal particulate detection"	1	1
1	"Metal particulate matter detection"	0	0
1	"Metal particulate detector"	0	0
1	"Metal particles detector"	8	2
1	"Metal particle detector"	37	7
2	Secondary references from Step 1		168
Total			329

Note: Several relevant results overlap across different search terms.

TABLE II
SUMMARY OF REQUIREMENTS FOR METAL PARTICLE DETECTION IN LYOPHILIZED VACCINE PRODUCT

Requirement	Specification
Speed	3-4 vials/min (manual), up to 400 vials/min (automated)
Volume	100% of vaccine vials
Test regiment	Non-destructive or selectively destructive
Particle Size	$>$ 100 micron (human), $>$ 10 micron (machine)
Integration	Inline analysis
Material	Stainless steel
Detection distance	$>$ Vial radius
Detection obstruction	Glass vial penetrating
Repeatability	Yes
Reliability	Yes

particle detection has never been published. In addition, the discussed reviews do not describe the physical properties of metals exploited for detection, which is key for understanding the working principles of metal detectors and further development of the field. In general, the properties of metals such as their high electrical conductivity, magnetic properties, or generation of eddy currents, which are essential for metal particle detection, are not explained in these review papers. As a consequence, building an understanding of the physical phenomena exploited by different sensing techniques allows an educated assessment of each method's merits.

In contrast to previous work, we provide a comprehensive overview of methods for metal particle detection. We further establish the requirements for successful metal particle detection in freeze-dried vaccines and discuss each detection methods' merits and disadvantages with regard to these requirements.

III. METHODOLOGY

We establish the requirements for inspection of freeze-dried vaccines by studying the relevant legal requirements (with a main focus on U.S. Government requirements for inspection) and inspection standards established in the industry and the research community. Finally, we include requirements based on the characteristics of freeze-dried vaccines that might only be implicitly considered in current inspection approaches.

To compile a complete picture of metal particle detection methods that we assess for metal particle detection in freeze-dried vaccines, we follow a two-step process. First, we search for papers on Google Scholar using a combination of search terms, as outlined in Table I, which yields 161 unique, relevant publications. Second, we included publications referenced in the results of our primary search, which discuss metal particle detection techniques. This step yields further 168 publications. We build a complete picture of current metal particle detection methods based on the publications that we identified and then assess them using the previously established requirements for the inspection of freeze-dried vaccines.

IV. REQUIREMENTS FOR THE INSPECTION OF FREEZE-DRIED VACCINES

Vaccine inspection with the goal of detecting metal particles needs to fulfill three main functions: 1) reliably detect metal particles within the relevant size range inside glass vials at sufficient distance; 2) not destroy or adversely affect vaccine quality; and 3) operate at sufficient speed and cost with reasonable resources. We discuss the requirements for metal particle detection in freeze-dried vaccines in the following chapter and present a summary of the requirements in Table II.

To aid our understanding of requirements for metal particle detection methods, we define what constitutes the typical metal particles that vaccine inspection seeks to eliminate. Government regulations dictate visual inspection of 100% of vaccine vials with the aim of an end product that is "essentially free" of particles [47], [48], [49]. Crucially, particles are defined by being unintentionally present in the vaccine, and they can consist of different materials, such as glass, fibers, and rubber, but, for the purpose of this article, we focus on metal particles. The main concern lies with particles of sizes greater than 10 μm, which are the subject of regulatory inspection standards [50]. To achieve vaccine vials essentially free of particles, inspection relies on unaided human vision under controlled conditions (e.g., light brightness and background color).

Human vision, therefore, sets the benchmark for any other inspection technology, and human limitations to inspection are crucial for assessing the merit of a proposed detection method. Human inspection is inherently probabilistic, detecting approximately 95% of particles at 200 μm, which rapidly declines to 40% of particles at 100 μm and further as particle size diminishes even under ideal inspection conditions in liquid vaccine product [51].

Due to stainless steel being widely used for vaccine production equipment [52], metal particles in freeze-dried vaccines are most likely to be of stainless steel as was the case in past recalls [20]. While other metals may possibly be present in vaccine production equipment, we focus our analysis on stainless steel, which is the most common wear particle that may be introduced to vaccines. A metal particle detection method, therefore, needs to detect stainless steel.

Quality inspection needs to keep up with the production process of vaccines. We consider the speed of inspection methods currently used in the pharmaceutical industry as a point

of comparison to assess methods. Manual inspection achieves an inspection speed of approximately 3 vials/min [16]. On the other end of the spectrum, automated inspection operates at a speed of approximately 400 vials/min [16]. Any metal particle detection method needs to perform at least comparable to these methods.

To achieve such high inspection rates, the detection system needs to be integrated with an automatic feed of vaccine vials, meaning that we require inline inspection to meet the requirements for speed and inspection of all vaccine vials simultaneously.

Furthermore, 100% of vials without defects cannot be inspected in a destructive fashion as no vials would be left for distribution. However, apart from nondestructive testing, an inspection method that is only selectively destructive for vials containing metal particles is acceptable as well.

Because the different regulatory requirements necessitate inspection as a last step before vaccines can be released from a production facility, the product needs to be inspected inside a glass vial. This means that not only does a metal particle detection method have to penetrate a glass vial but it also needs to be able to detect metal particles at a distance of at least half the vial diameter, which can vary but is typically on the order of a few centimeters.

Last but not least, any metal particle detection method needs to yield repeatable measurements under the same conditions and over time.

V. Discussion of Metal Particle Detection Methods Their Shortcomings and Benefits for Vaccine Inspection

Metal detection methods typically involve sending a physical signal, such as acoustic or electromagnetic waves, to the sample. The interaction between the metal particles and the signal is then measured using a sensor. We believe that an essential future trend of work will involve exploring the limits of the detection of metal particles in vaccines, considering factors such as their size and depth. Since these limits are strongly influenced by the type of the signal detected and the materials present in the sample, a classification of methods based on the nature of the signal detected would greatly aid the advancement of the field. Consequently, we categorize metal detection methods into five primary groups: 1) acoustic methods; 2) electric methods; 3) magnetic methods; 4) optical methods; and 5) electron-based methods. Each group leverages specific properties of metals, which we will explain further. In addition, there are four outlier techniques that rely on different principles: 6) mass spectrometry; 7) gravimetric analysis; 8) the thermal product sensor; and 9) the resonance frequency shift method. To summarize our analysis, we provide a visual representation in Fig. 1. For each metal particle detection method, Fig. 1 outlines the type of signal used for metal particle detection, the detectable particle size, whether or not the method is applicable to the inspection of freeze-dried vaccines, and the main type of information the method provides about detected metal particles.

We begin with a brief analysis of the suitability of methods 6)–9) in freeze-dried vaccines. Mass spectrometry provides the quantitative and qualitative elemental composition of the sample [53], [54], [55], [56], [57] and, as a consequence, can detect metals [54], [57], [58]; however, it requires atomizing and ionizing the sample, making it inapplicable in a vaccine. In gravimetric analysis, a liquid sample is passed through a membrane [41], and the remaining debris is weighed, making it also inapplicable in a vaccine. The thermal product sensor [59] can generate false alarms due to water or noise and requires the sample to be in contact with the sensor. In addition, it has only been tested with liquids. Hence, it is not a recommended choice for vaccine inspection. The sensor based on resonance frequency shift measures a variation of the resonance frequency of a cavity due to the presence of a particle, which has allowed the detection of metallic objects inside a cavity [60], [61], [62]; however, it seems inapplicable for detecting metal particles in a freeze-dried vaccine.

A. Acoustic Methods

Metal detectors relying on measuring acoustic waves can be classified into the collision-based acoustic method, ultrasonic sensors, and scanning acoustic tomographs.

The collision-based acoustic method employs a target such as a grounding electrode in order to attract ferrous particles and uses the acoustic signal generated when the particles collide with the target for obtaining information about the number and size of the particles [35], [63]. However, it can only be used when the viscosity of the material allows the particles to reach the electrode at a large enough speed, which would not be the case in a freeze-dried vaccine.

The ultrasonic sensor relies on the change of acoustic properties of the sample, such as acoustic reflection coefficient, due to the presence of solid debris. It is composed of an ultrasonic transmitter and a receiver; the transmitter sends an ultrasonic wave that penetrates the studied substance; and the receiver detects the reflected or the transmitted wave. If solid particles are present in the channel, they scatter the ultrasonic wave and attenuate the transmitted wave. Thus, the measure of the transmitted or reflected waves can indicate the presence of particles and their number and size [64], [65]. Ultrasonic sensors have been used in oil analysis [64], [66], [67], [68], [69] and can detect, count, and measure particles in oil with sizes ranging from 3 to 2000 μm in concentrations between 0.01 and 12.8 ppm [66]. In addition, the method can distinguish solid particles from air bubbles and water droplets due to differences in the scattering properties of these materials [66], [67]. However, the sensor cannot distinguish metal particles from nonmetal particles when they have a similar behavior under acoustic waves; temperature, sample viscosity, flow speed, and mechanical vibration may affect the performance of the ultrasonic sensor, limiting most of its real-life applications in oil analysis [31], [32]. Ultrasonic sensors have been used for the analysis of surface or subsurface defects in solid objects such as metals, plastics, or wood [70], in food [71], and in bottled beverages [72]. Hæggström and Luukkala [71] employed ultrasound reflection measurements in cheese and marmalade and detected 1-mm steel particles at a 75 mm depth. However, the signal-to-noise ratio (SNR) decreased in nonhomogeneous samples, reducing the maximal

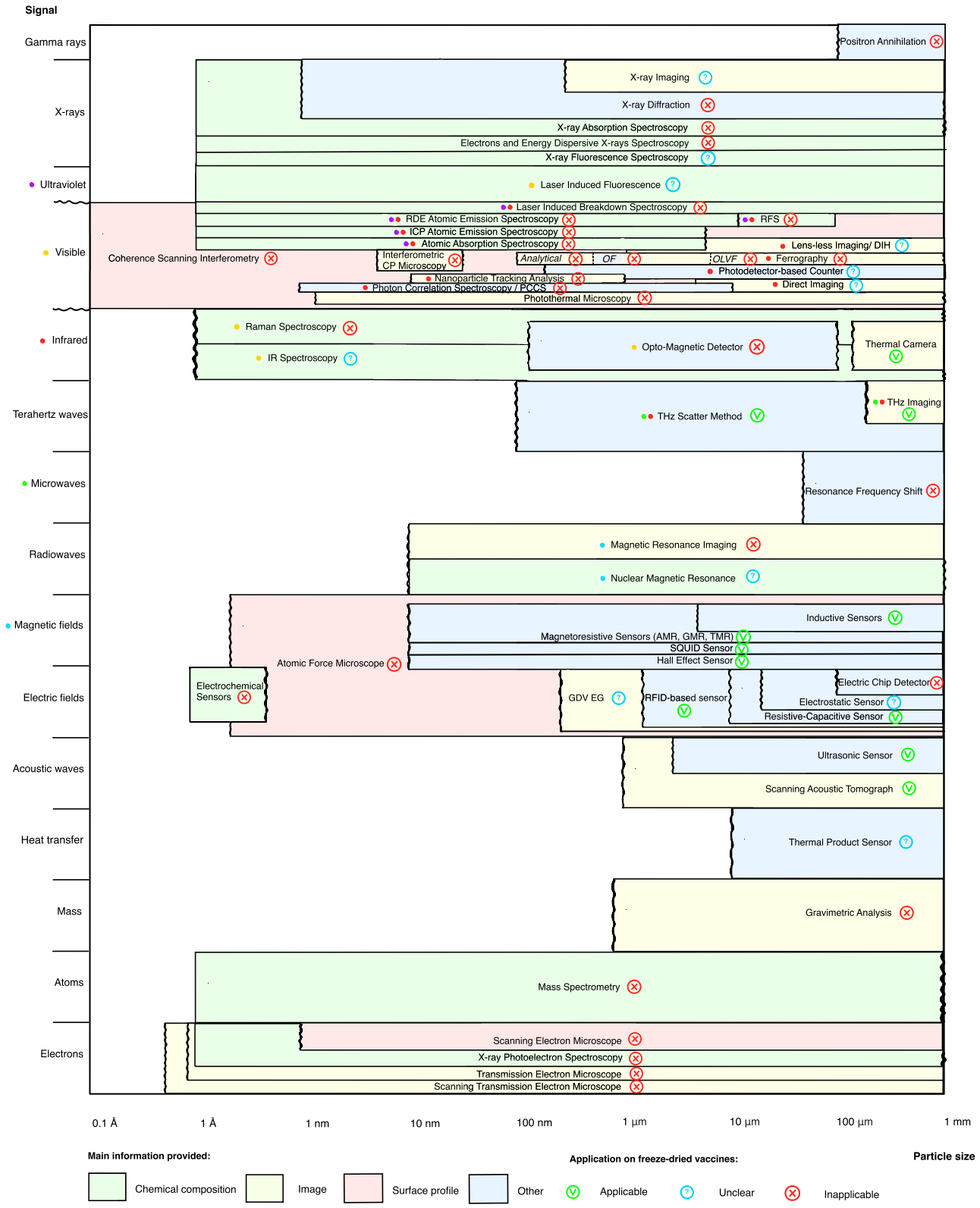

Fig. 1. Summary of metal particle detection methods. Method applicability refers to metal inspection of freeze-dried vaccines and is based on comparing reported methods with mass inspection requirements as described in the text. When the literature does not provide enough information, as in the case of the thermal product sensor, we have marked them as unclear. Particle size refers to the spectrum of particle sizes that can be detected through each method. It does not exclusively correspond to the detection of individual particles; for instance, magnetoresistive, Hall, and SQUID sensors have reportedly identified clusters of magnetic particles measuring around 10 nm. In cases where the detection limit is ambiguous, we have estimated it through our analysis and represented the limits with curved lines. No supporting experiments in vaccines have been described in the literature, and depth detection needs to be established before validating depicted choices. Some methods, such as mass spectrometry, may be applied but only in samples that are destroyed.

detection depth. In [72], particles of different metals and different sizes (larger than 1 mm) were detected in bottled beverages.

An image of the sample can be obtained through scanning acoustic tomography, which represents a fast and nondestructive technique for detecting defects such as delamination, cracks, voids, or changes in density in materials. It achieves very high resolution, detecting internal defects as small as 1 μm [73]. However, air highly attenuates ultrasonic waves [74], which necessitates the use of contact measurements, thus resulting in higher inspection times. A solution was proposed for performing noncontact ultrasonic sensing in food [75]; however, only particles larger than 2×2 mm^2 were detected. Note that ultrasonic detectors have not been reportedly used for detecting metal particles in freeze-dried vaccines, and it is not clear if the difference of the acoustic properties between metallic particles and the freeze-dried vaccine cake allows for the detection of metal particles. Hence, future research is necessary in this area.

B. Electric Methods

Electric methods can be classified into electric chip detectors, electrostatic sensors, resistive–capacitive detectors, radio frequency identification (RFID)-based detectors, electrochemical sensors, and gas discharge visualization electrography (GDV EG).

Electric chip detectors are inapplicable in vaccines due to their working principle. They are used in channels with oil flow; a magnetic field leads to accumulation of ferrous particles on the surface of two electrodes; once they reach a certain amount, they bridge the gap between the electrodes and generate a signal [76].

The electrostatic sensor detects charged particles and is able to sense charged microparticles with diameters down to 20 μm in an oil channel with a flow rate up to 9 L/min [77]. The sensor is robust, provides real-time detection, and is relatively inexpensive [78]. The method relies on the fact that charged metal particles passing through the detection zone induce the presence of the same amount of opposed charge in the probe. However, the ring probe is not sensitive to particles placed in the center of the channel [79]. Research to improve the sensitivity of the electrostatic sensor has investigated [78], [79], [80], [81], the effect of sensor parameters on its detection sensitivity [79], and the benefits of signal processing [81]. Since a single electrostatic sensor exhibits inhomogeneous sensitivity, Tang et al. [78], [80] developed a hemisphere-shaped electrostatic sensor with a circular array yielding a more homogeneous sensitivity. The device was later improved using the compressive sensing algorithm [78]. The electrostatic sensor is limited due to external interference and noise highly affecting its performance, and its use on vaccine inspection depends on whether metallic debris in vaccines is charged, which is unclear and should be further investigated.

In the resistive–capacitive method, two electrodes are placed on opposite sides of a small channel, generating an alternating electric field. A particle passing through the electrodes with different conductivity or permittivity from the filling medium will produce a resistance or capacitance change in the poles, generating a signal. The method has been primarily used in the detection of wear debris in oil [36], [82], [83], [84], [85], [86], [87], [88]. Since the capacitive approach allows the detection of relatively conductive particles in a nonconductive medium [84], it can be applied to other nonconductive samples such as vaccines. The capacitive sensor can detect and count metal particles as small as 10 μm in lubricating oil flowing inside a 40 μm (H) $\times$ 100 μm (W) channel with a flow rate of 70 μl/min [36]. In order to increase sensitivity, Islam et al. [87] developed a high-precision cross-capacitive sensor providing the exact relation between capacitance and permittivity of the studied medium. In order to decrease the particle size detection limit, Murali et al. [36] employed a microfluidic capacitive sensor; however, this results in a lower throughput and a lower detection size range. A solution to this problem is the use of sensors employing multichannels, such as studied in [85]. The use of silicon steel sheets, which enhance electric field lines, also improves sensitivity without reducing throughput [89]. The resistive–capacitive method has three main drawbacks: 1) ferrous and nonferrous metal particles cannot be distinguished since their permittivity is almost equal, making their response to an electric field very similar; 2) the signal is affected by the chemical state of the sample [31], and other particles with permittivity different from that of the sample (e.g., air bubbles and water droplets) can also cause capacitance pulses leading to false alarms; and 3) in the case of oil analysis, the applied electric field accelerates oil deterioration, which, in turn, affects the dielectric permittivity of oil [32] and can cause measurement errors. Hence, whether the electric fields can affect the state of the vaccines should be analyzed.

The RFID-based detector employs an RFID system—generally consisting of a tag or transponder, a receiver, and a transmitter. The presence of metal particles disturbs the electromagnetic properties of the sample—such as electrical conductivity and magnetic permeability—which, in turn, affects the performance and characteristics of the system antennae [90], [91]. As a consequence, RFID systems have been used as sensors for detecting the presence of metal particles [92] and cracks in a metal structure [93]. Yin and Ren [92] placed an oil sample between the tag and the receiver, and detected the presence of ferrous particles and their amount; 2–3-μm iron particles at a total mass between 0.5 and 2.0 g were detected in a 40 mm (D) $\times$ 50 mm (H) glass container filled with oil. Note that future research is expected in order to reduce the noise and improve accuracy.

In electrochemical sensors, the sample reaches a sensing electrode where an electrochemical reaction occurs, and the signal is transformed into an electric signal, providing information about the concentration of specific ions. Hence, electrochemical sensors have been used for detecting metal ions [39], [94], [95], [96] in food [94], aqueous solutions [39], and blood [96]. Metal ions can be detected through electrochemical stripping analysis; however, this requires the accumulation of the target analyte or a compound of the target on a working electrode [97], which cannot be performed in vaccine inspection. In addition, only metal ions and not large metal particles seem detectable through electrochemical

sensing, making it inapplicable for detecting large metal particles in vaccines.

GDV EG relies on the Kirlian effect and is based on the detection with a digital camera of the electrical discharge or radiation emitted by the sample after the application of a high-frequency high-voltage current [38]. It has been used for detecting metal nanoparticles in water [38]; however, its suitability on freeze-dried vaccines has not been studied, and therefore, its possible application in vaccines is unclear. Notice that the method has been classified an electric detector since it is based on electrical discharge and the emission of electric fields by the sample.

C. Magnetic Methods

Metal particle detectors relying on measuring magnetic fields can be classified into three main methods: 1) the radio frequency (RF) approach, which involves sending RF-electromagnetic waves and using a magnetic sensor to measure the perturbation of the magnetic field by the metal particles; 2) the direct-current (dc) approach, where the sample is exposed to a static magnetic field and a magnetometer measures the distortion caused by the ferrous particles; and 3) NMR and magnetic resonance imaging (MRI), which involve exposing the sample to both dc and RF fields and measuring the magnetic field produced by the atomic nuclei of the sample.

Due to the high penetration of magnetic fields and RF waves in biological materials, magnetic detectors are one of the best choices for detecting metals inside a vaccine. We first introduce the main physical effects that lead to the detection of metal particles by magnetic methods.

These effects are mainly the eddy current effect and the magnetization effect, both resulting in the generation of new magnetic fields. The eddy current effect arises in metals due to their high electrical conductivity, attributed to the presence of free electrons that move easily within the material. When subjected to a time-varying magnetic field, these free electrons create eddy currents, generating a magnetic field opposing the external one. Eddy currents only appear in sufficiently conductive materials, and thus, they should be generally weaker in the vaccine cake compared to a conductive metal. On the other hand, the magnetization is only significant in ferrous metals such as iron, cobalt, nickel, gadolinium, and alloys. It results from specific atomic arrangements and magnetic moment interactions, causing the alignment of the moments of magnetic domains when an external magnetic field is applied, leading to the generation of a new magnetic field in the same direction. Note that stainless steel, which is the main metal of interest in vaccine inspection, is a relatively good conductor of electricity; however, its magnetism depends on the specific phase. For instance, in the martensitic phase, it displays a ferromagnetic nature and a robust remanent magnetization, while, in the austenitic phase, its remanent magnetization is comparatively weaker.

The RF approach takes advantage of both eddy current and magnetization effects. It involves using a magnetometer to measure time-varying magnetic fields. The most common application of this method relies on the use of an inductive sensor due to its several advantages. Therefore, we provide in the following a review of the RF method performed with an inductive sensor, which we will simply call the "inductive method" for convenience.

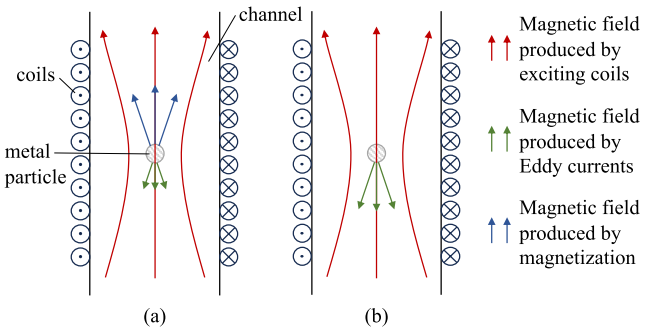

Fig. 2. Working principle of the inductive method, where an alternating magnetic field is applied on the sample. (a) Ferromagnetic metal particle: although both eddy current and magnetization effect take place, the magnetization overcomes the eddy current effect, leading to an increase in the magnetic flux in the sensing zone. (b) Nonferromagnetic metal particle: the eddy current effect dominates, reducing the magnetic flux in the sensing zone.

In the inductive method, exciting coil(s) generates an alternating magnetic field inside the channel, which induces the generation of a new magnetic field by metal particle passing through the detection area, due to the eddy currents and the magnetization effect. Fig. 2 illustrates the working principle of the inductive method; in ferrous metal particles, the magnetization effect overcomes the eddy current effect, while, in nonferrous metal particles, the eddy current effect is predominant. Hence, nonferromagnetic metal particles locally weaken the magnetic field, while ferromagnetic particles enhance it, leading to opposite changes of magnetic flux in the sensing zone. Therefore, the phase of the signal for nonferrous metal particles is opposite to the one of ferrous particles, allowing their distinction. In addition, the method presents several advantages such as being contactless, nondestructive, consisting of a simple structure, providing a rapid analysis [99], and functioning under high temperatures and vibrations. Due to the high penetration of radiowaves in most materials, it can detect metal particles underground or snow and in food [100], [101], textile materials and paper [102], juice [103], lubricating oil [86], [89], [99], [104], [105], [106], [107], [108], [109], [110], [111], [112], [113], [114], [115], [116], [117], [118], [119], [120], [121], [122], [123], [124], [125], [126], [127], [128], [129], [130], [131], [132], [133], [134], [135], [136], [137], [138], [139], [140], [141], [142], [143], [144], [145], [146], [147], [148], [149], [150], [151], [152], [153], [154], [155], [156], [157], [158], [159], [160], [161], and inside a closed hand [162]. The inductive method can detect an iron particle as small as 5 μm in oil in a 1-mm diameter solenoid [149] and a copper particle as small as 20 μm in a coil with a 0.3 mm inner diameter [131]. However, commercialized inductive detectors have a higher detection limit, e.g., the debris sensor developed by GasTOPS can detect in oil a 125-μm diameter ferrous particle and a 450-μm diameter nonferrous particle using a 8-mm sensor bore and at

a flow rate up to 12 L/min. It is also important to note that the method is insensitive to air bubbles, water droplets [108], and nonmetal particles. To determine the material composing the detected particle, Flanagan [104] performed the demodulation of both frequency and amplitude of the signal independently, obtaining two output voltages and allowing an estimation of the material based on a locus diagram. In addition, the amplitude of the signal is proportional to the mass for a ferrous particle and to the surface area for a nonferrous particle [43].

In general, inductive sensors do not provide the location of the particles. In order to overcome this problem, Chady et al. [163] used an electromagnetic tomography system relying on multiple transducers and giving the 3-D location of metallic objects, and Suzdaltsev and Lobanova [164] proposed a metal detector based on three transducers placed at different angles from the sample, giving the location of the metal particle.

Extensive research has been carried out in order to increase the sensitivity of inductive detectors [31], [32], [33], [34], [89], [110], [112], [113], [114], [115], [120], [122], [124], [127], [134], [135], [136], [149], [152], [165], [166], [167], [168], [169], which is mainly realized by increasing the strength of the magnetic field in the channel and decreasing the particle-sensor distance. These two approaches can be performed in various ways, such as using microfluidic channels [124], multichannel-based sensors [112], [152], [170], placing multiple sensing coils inside the channel [169], using multilayer sensing solenoids [149], adding silicon sheets [89], [135], and ferrite cores to the sensing coils [136], [168]. The SNR can also be increased by adding a capacitance to the coils and working in a resonant state [113] and with the use of signal processing algorithms [149], [165], [166], [167]. Detection sensitivity of nonferrous particles can be improved with the addition of resistance detection [134], [136], with the increase in excitation frequency [122], and with the reduction of particle velocity [120], [127]. On the other hand, it is easier to detect ferrous particles as the frequency decreases [122].

The inductive method has several drawbacks: 1) the magnetic fields produced by ferrous and nonferrous particles may cancel each other out, rendering the particles undetectable; 2) multiple small particles can be interpreted as a single larger particle; and 3) commercialized inductive sensors fail to detect metal particles smaller than 60 μm.

Compared to RF magnetic fields, static magnetic fields have several advantages; notably, they eliminate the skin effect, which can lead to an increase in temperature and distortion of the magnetic field, and they simplify the drive circuit and are more resistant to interference [171]. Hence, metal detectors employing static magnetic fields have also been investigated [42], [142], [172], [173], [174], [175], [176]. Under this approach, a static magnetic field is applied to the sample, and the magnetic fields produced by the magnetized particles are measured during or after its application. Since the property that is being probed is the magnetization of particles, only ferrous particles can be detected. The perturbation of the magnetic fields is measured with magnetometers such as SQUID, Hall effect, magnetoresistive sensors, inductive coil, nitrogen-vacancy diamond (NVD) magnetometers, spin exchange relaxation-free (SERF) magnetometers, and others [177], [178]—for an extensive review of magnetometers, we recommend consulting [178]. The general working principle of the dc magnetic method is represented in Fig. 3.

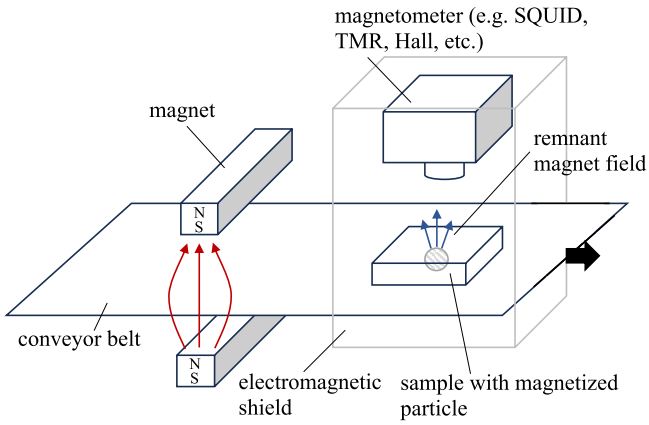

Fig. 3. Schematic of the dc magnetic method for metal particle detection. A sample is moved on a conveyor belt first through a pair of magnets, which is used to magnetize ferromagnetic particles in the sample. The sample is then moved under an electromagnetic shield where a magnetometer measures any remnant magnetic fields from the magnetized particles in the sample. Adapted from [98].

Using the dc method based on inductive coils [142], [173], [174], [175], [176], the detection limit lies at 13 μm for iron particles using the high-gradient magnetic field method, with a 40-mm-diameter and 100-mm-long oil channel and at a flow rate of 3.75 L/min [175].

The other main magnetic sensors that have been reportedly used for detecting metal particles under the dc method are SQUID, Hall effect, and magnetoresistive sensors. Although these sensors have mostly been used for the detection of magnetic beads in biosensing, they present a promising approach for industrial inspection of vaccines. In addition, the deconvolution of the magnetic responses under a certain range of external magnetic fields can allow the distinction of different types of magnetic nanoparticles and the detection of their fractional ratios within a mixture [179]. Combining the measurements with magnetorelaxometry, different types of nanoparticles can be distinguished based on their different relaxation times [180]. We discuss next the main benefits, drawbacks, and reported applications of these sensors in detecting metal particles.

SQUID sensors are the most sensitive sensors to magnetic fields in a wide frequency range, from dc fields to frequencies up to a few GHz [177], and have achieved the detection of a single ~120-nm nanoparticle [181] placed near the edge of the sensor. The SQUID sensor has been applied in biosensing [182], [183], [184], [185], MRI [177], [186], food inspection [98], and industrial product control [187]. Krause et al. [187] detected a 0.09-mm stainless steel particle in industrial products with and without aluminum wrapping. Tanaka et al. [98] used three high-Tc RF SQUID sensors for finding small steel particles with 0.3–0.8-mm diameters in food in sample volumes up to 150 mm (W) × 100 mm (H). The stand-off distance was 117 mm, the conveyor moved at 20 m/min, and

the signal was approximately proportional to the volume of the particle in the studied range of sizes. Moreover, the signals were not affected by other electromagnetic fields due to the use of electromagnetic shields [98]. In order to ensure high sensitivity in relatively wide areas, Tanaka et al. [188] used a two-channel high-Tc SQUID gradiometer system composed of two planar high-Tc SQUID gradiometers for detecting the remnant magnetic fields from iron particles in lithium-ion batteries. A single SQUID gradiometer detected 40–75-μm diameter iron balls on a conveyor belt at a speed of 6 m/min at a 3 mm distance from the SQUID gradiometer. The two-sensor system was able to detect an iron particle of 100×100 μm^2 surface and 50 μm thickness at a liftoff distance of 3 mm and at a detection width of 22 mm. The inspection can also be improved to obtain an image of the sample by scanning the sensor over the sample surface, such as performed in [189], where the authors used a remanence-based SQUID sensor and detected 25-nm magnetic particles in tissue at 1.7 cm distance from the sensor with a sensitivity of 10 ng and a spatial resolution of $\sim$1 cm. However, SQUID sensors have to be used under very low temperatures [177], [185], [190] in order to achieve superconductivity, making their application in industrial environments difficult.

Hall effect sensors measure static or alternating magnetic fields with frequencies below $\sim$1 MHz [191] and are generally small, light, and inexpensive devices, requiring low power and operable at a wide range of temperatures [191]. They can detect magnetic particles [179], [192], [193], [194], [195]; however, they are limited by their low sensitivity.

Magnetoresistive sensors are, in general, less sensitive than SQUID sensors. They measure magnetic fields through the use of simpler devices requiring low power and without the need for ultralow temperatures. These sensors rely on the magnetoresistive effect, i.e., the change of electrical resistance of a ferromagnetic material due to the change of the magnetic field. The three main types of magnetoresistive sensors are anisotropic magnetoresistive (AMR), giant magnetoresistive (GMR), and tunneling magnetoresistive (TMR) sensors, and they can detect nanoparticles with sizes down to $\sim$10 nm [196] on the surface of the sensor at large enough concentrations. AMR sensors have a simpler structure than GMR and TMR, and have been used for detecting superparamagnetic particles [197], [198]; however, GMR and TMR sensors can achieve higher sensitivity. The use of GMR sensors for biosensing, in order to detect magnetic nanoparticles labeling specific antibodies, has been studied previously [45], [185], [196], [199], [200], [201]. Compared to commercialized inductive techniques, magnetoresistive sensors consume less power, are less complex, and present better portability [202]. However, it is difficult to use GMR sensors for noncontact measurements; in general, magnetic nanoparticles have to be kept at a small distance from the sensing unit since the GMR signal rapidly decays over distance [202]. Furthermore, the presence of noise in low-frequency fields [45] further limits the sensor. TMR sensors present advantages over traditional Hall sensors, AMR, and GMR sensors, such as higher sensitivity, working under a wider range of temperatures, and resistance to mechanical shock and vibration [203]. TMR sensors have been used for detecting magnetic particles in biosensing [45], [185], [202], [203], [204], [205] and present advantages over traditional optical sensors such as being able to overcome the interference of background color and light with complex samples, high sensitivity, and accurate quantification [203]. In addition, compared to fluorescence signals, the magnetic signal emitted by magnetic beads suffers less from attenuation and is more stable [203]. TMR sensors are able to overcome environmental interference and can, thus, be applied to many different samples, such as water, food, and blood [203]. They have also been used for detecting 1-mm iron particles in manufacturing environments [206], and electromagnetic interference can be greatly eliminated using the matched filtering technique, resulting in an increase in detection sensitivity [206]. However, the TMR sensor is limited by sensitivity to noise and complex fabrication [45].

In NMR, a static magnetic field and an orthogonal alternating magnetic field are applied on the sample, and as a result, the electromagnetic waves produced by the atomic nuclei are detected. NMR can be used for the detection of debris such as metals in a fluid such as oil, water, or fuel [207], either by detecting the spectrum produced by an element such as ^1H and detecting perturbations of the spectrum due to the presence of contaminants or by directly measuring the signal generated by the metal particles [207]. It is possible to obtain 3-D information of the sample using high-gradient magnetic fields—in this case, the method is known as MRI. Either using NMR or MRI, it is possible to detect the presence of small metal particles, down to sizes in the nanometer range [208]. NMR and MRI have been applied in the medical field for detecting metals [208], [209], [210], [211], [212], and metal objects can be detected because they cause intensity changes of the MRI image [211] and image anomalies [213], [214]. However, MRI remains a high cost and time-intensive technique, making it inapplicable for inline inspection of vaccines.

Note that measurements of the magnetic properties of the sample can also be obtained with magnetic force microscopy, which has allowed the detection of metallic molecules in biological samples [215]; however, it cannot be performed offline; it only provides information about near-surface particles and requires direct contact with the sample.

D. Optical Methods

Optical detection methods rely on detecting light and can be classified into: 1) photodetector-based sensors; 2) imaging sensors; 3) spectroscopic analysis techniques; and 4) ferrography.

1) Photodetector-Based Sensors: Photodetector-based sensors rely on measuring variations of light flux and correlating them to the amount of particles. In the area of oil condition monitoring, photodetector-based sensors counting the number of particles have been developed. The most simple optical counter is based on light obscuration [42], [216], relying on the blockage of visible light by opaque particles. The use of a light slit instead of a collimated beam provides a higher SNR [42]. However, a high sensitivity implies the use of small channels, reducing the size detection range. A higher sensitivity is

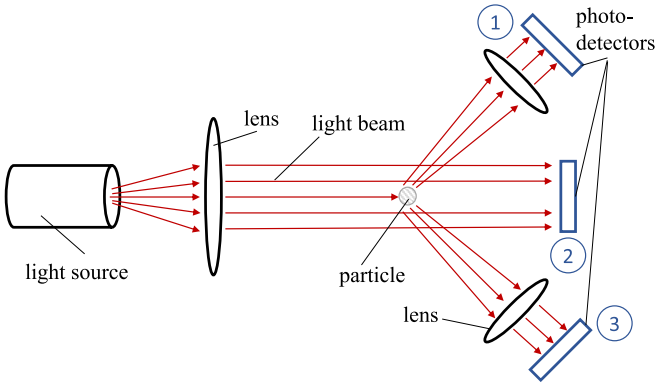

Fig. 4. Schematic of the photodetector-based method. Light in the visible spectrum, IR, or THz is used. Photodetectors ① and ③ detect light scattered by the particle, and photodetector ② detects the transmitted light. A sensor using only detector ② relies on the principle of light obscuration.

achieved in particle counters based on light scattering [42], where the photodetectors are placed at different angles and the scattered light is detected. The working principle of the photodetector-based method relying on the principles of light scattering and light obscuration is illustrated in Fig. 4. Optical counters from Rio based on light scattering can detect particles with sizes from 0.2 to 2 μm. Particles in a wide size range can be detected with the optomagnetic detector based on the formation of chains of ferrous particles in a liquid under the application of a magnetic field. It can detect ferrous particles in oil with sizes from $\sim$1 nm to $\sim$100 μm [35]. In liquids, the light scattered by moving particles also yields key information using Doppler anemometry [217], [218], photon correlation spectroscopy (PCS) [219], [220], and photon cross correlation spectroscopy (PCCS) [221]. However, Doppler anemometry, PCS, and PCCS are inapplicable in freeze-dried vaccines. In order to detect metal particles in opaque samples, it is preferable to use light in wavebands other than visible light. IR rays have been used for detecting wear debris in dirty oil [35], and THz radiation presents unique properties making it the source of new and promising methods for detecting metal particles.

THz waves present several advantages, such as being non-ionizing, noninvasive, and spectral fingerprinting [222], and having a high penetration in nonconductive and nonpolar materials, such as plastic [223], graphene [224], pressboard [225], paper, clothes, cardboard, ceramics, wood, and some food products. Since metals strongly reflect THz waves, THz detection allows an easy distinction of conductive particles in a nonconductive material [223]. However, water also strongly reflects THz waves, making THz sensors inapplicable in aqueous solutions. Using a transmitter and a receiver antenna and detecting the scattered THz radiation, Kitahara et al. [223] detected a single 300-μm stainless steel particle on a plastic film, but smaller particles were not detected since the intensity of the scattered light and the SNR ratio greatly diminished with particle diameter [223]. Yang et al. [224] proposed a rapid and accurate method providing the concentration of metal nanoparticles in a nonpolar material based on a THz time-domain spectroscopy (TDS) system. The method detected nanosilver particles with an average diameter of $\sim$100 nm in a graphene film [224] and relies on the fact that the used particles scatter THz waves according to Rayleigh scattering, which yields a linear relation between the transmitted THz amplitude and the concentration of particles. However, thicker samples could have a less predictable influence on the transmission amplitude of the THz waves, and thus, the reliability of the method could decrease in thicker samples. The effectiveness of THz detection in vaccines depends, among other factors, on whether enough radiation can be transmitted through the whole vaccine, which should be further studied. Gamma rays can achieve high penetration and can, thus, be used in thick samples. The sensor developed in [226] detects gamma rays produced by positron annihilation and allows the nondestructive detection of metal particles and other impurities in liquids confined in relatively thick pipes, such as 30-cm aluminum tubes or 10-cm stainless steel tubes [226]. However, the method implies injecting positron nuclide in the sample, is only applicable to liquids, and can damage the sample.

2) Imaging Sensors: Imaging techniques that have been used for detecting metal particles can be classified into: 1) microscopic techniques that are only performed offline and 2) detectors that can be used online, mainly digital shearography, direct imaging, lensless imaging, hyperspectral imaging with IR/near IR (NIR), thermal imaging, THz imaging, and X-ray imaging.

Metal particles have reportedly been detected with microscopy techniques, such as photothermal microscopy [227], [228], [229], [230] and interferometric cross-polarization microscopy [231]; however, these methods are only performed offline. Dark-field microscopy [232] and nanoparticle tracking analysis have also been used, but they are only applicable on the surface of liquids and cannot be performed inline.

Direct imaging sensors use the light blockage by opaque particles for providing images of relatively transparent samples; they can be applied in inline inspection and can detect and count particles in oil as small as 5 μm in a 100-μm-thick sample [233]. However, if a high resolution is needed, the field of view (FOV) and the depth of view have to be kept sufficiently small [234], limiting the inspection of large volumes. The lensless sensor takes advantage of the diffraction of light caused by particles and can achieve a higher depth of view. For instance, it can reach resolutions around 2 μm in large sampling volumes (FOV: $\sim$20 mm^2 and depth of field (DOF): $\sim$1 mm), detecting particles in the sample based on the shadows that they generate [234]. In biological samples, such as blood, 3-μm particles can be detected with a resolution around 1–2 μm and an FOV of $\sim$25 mm^2 [235]. The lensless sensor in the coherent mode, also known as digital inline holography (DIH), enables a further reconstruction of the holographic images in order to resolve the original particles with resolutions below 1 μm [234], providing the size, 3-D position, and velocity of particles [236]. DIH has been used for detecting aluminum particles in combustion [236] and wear particles in lube oil [234], as well as tracking particles in multiphase flows [237]. In [234], DIH was combined with

stroboscopic illumination. As a result, wear particles were imaged and detected with a field-of-view of 5.5 mm × 4.1 mm, depth of view of 500 μm (for ∼70 μm particles), and a resolution of 2.5 μm/px, with a flow rate around 1–3 L/min [234]. Although the direct imaging sensor and the lensless sensor typically employ visible light, they could be used with THz waves in order to detect metal particles in an opaque vaccine. However, their working principle using THz waves might change (e.g., in the case of the lensless sensor, a diffraction of THz light different from the diffraction of visible light by opaque particles could lead to a slightly different technique). Hence, their possible application in a vaccine is unclear.

THz-based cameras allow the detection of metallic objects in industrial packaging [238], security screening (e.g., detecting a knife behind a newspaper [239]), and food [240], [241], [242], [243], e.g., inside a chocolate bar [244]. However, the spatial resolution of THz cameras is on the order of some hundred micrometers [243]. The use of a horn antenna has been proposed for increasing the spatial resolution [240]; however, the obtained resolution was still over 500 μm. THz pulsed imaging (TPI) has been used in the pharmaceutical field [245] for determining the uniformity of tablet coatings and measuring their thickness [245], [246], and presents advantages such as employing extremely low power and being insensitive to air bubbles [245]. In TPI, ultrashort pulses of THz radiation are sent to the sample and partially reflected back at each interface [246]. However, the optical delay has to be scanned mechanically at each pixel, which results in a slow acquisition [247], leading to the inspection of an entire tablet requiring tens of minutes [245], which, although faster than X-ray micro-computed tomography (CT), is still time-expensive for inline application. A solution to this problem was proposed with the use of a quantum cascade laser and a scanning mirror, providing an image of ∼40 mm diameter in 1.1 s [248], obtaining an image of dimension 77 × 70 pixels. In addition, using CT and combining the projection images obtained at different angles, the authors obtained 3-D images of an ellipsoidal sample with axes of ∼40 mm within 87 s. However, the analysis was not aimed at the detection of particles. Palka et al. [225] used a THz-TDS system, rastered the THz beam over the surface, and, as a result, detected ∼300-μm metal particles in the middle of 2.5-mm-thick pressboard samples, with an acquisition time of 0.3 s per pixel. In addition, since the sizes of the spots caused by the presence of metal particles were much bigger than the actual particles, the imaging process could potentially be performed more rapidly using larger step size, providing a more easy detection than using X-rays, where the spots are smaller [225]. Indeed, THz imaging provides higher contrast than X-ray imaging [29]. In order to provide high sensitivity while keeping a fast acquisition, Ok et al. [241] developed a continuous-wave sub-THz transmission system with a polygonal mirror for scanning, which yielded a faster analysis than prior sub-THz transmission imaging systems. The system achieved a scanning speed of 80 mm/s and a resolution of up to 2.83 mm, and according to the authors, a higher imaging speed can be acquired with the use of image processing algorithms and digital signal processing [249], [250], [251]. For some applications, THz equipment cost needs to be addressed before its commercial use is viable [252], [253].

IR cameras have also been used for detecting metallic objects as small as 2 × 2 mm on the surface of pork steaks using hyperspectral imaging [254], which provides both an image and chemical information. However, the penetration of IR is limited, and its use in freeze-dried vaccines has not been studied. The IR radiation emitted by metal particles can be enhanced with the application of RF waves, which induce eddy currents in metallic materials and, in turn, raise their temperature [255]. A thermographic camera is then used in order to collect the emitted radiation. The detection of metal particles based on thermographic cameras and induction heating coils has been previously studied [190], [255], [256], [257], [258], [259], [260], reaching the detection of a 0.15-mm-diameter stainless steel particle in a ∼0.01-mm-thick high-performance chemical film [256]. Its use would probably harm the vaccine but only under the presence of metal particles.

In X-ray imaging, X-rays are sent through the sample, and the transmitted or scattered rays are detected. The penetration rate of X-rays decreases when the product of the atomic number and density increases [261], which makes metals such as iron or copper much less transparent to X-rays than many materials such as food or plastic. In addition, density changes can be detected due to changes in the gray values in the resulting images [262], allowing the detection of metal particles. X-ray imaging has been performed for detecting metal particles in food [261], [263], [264], [265], plastic [266], and biological tissue [267] using dark-field radiography [268], [269], [270]. X-ray imaging can detect metal particles as small as 0.3 mm in dry packaged food [264]. The X-ray inspection devices commercialized by Anritsu can detect ferrous and nonferrous metals, with diameters as small as 0.3 mm in dry products and as big as 240 mm (W) × 120 mm (H) and at a belt speed up to 80 m/min. However, X-ray imaging may be unable to detect metal particles producing little to no shadow, such as extremely thin particles or aluminum [267]. X-ray transmission imaging has been used on planar samples allowing the detection of a 20-μm metal particle in plastic [266]. To increase the sensitivity of X-ray imaging, the dark-field mode has been developed, being in some cases more sensitive than transmission imaging [269]. The resolution can also be increased through microfocus X-ray radiography, using a very small focal spot, which provides a higher resolution than conventional systems [271]. Due to its high penetration capabilities, X-ray has been used in the reconstruction of relatively large volumes, namely, through X-ray CT (XCT), providing 3-D information. XCT has been performed in biological objects [272], [273] and in fluids containing particles [274], achieving the reconstruction of the head of a mouse with a resolution of 7.6 μm and a scanning time of 73 s [272]. Since metals have a higher density than bone and biological tissues, variations in light attenuation can allow their detection, making XCT a promising technique for detecting metal particles in large volumes. X-ray micro-CT can achieve higher sensitivity, reaching resolutions in the submicrometer range [275]. It has been used for the nondestructive

characterization of food [262]; however, it requires long run times and small samples, which makes it currently inapplicable in rapid industrial inspection. More generally, in X-ray imaging, higher sensitivity results in longer running times (e.g., over an hour in [273]) and depends on the sample size: for a 100-mm sample, the resolution will be 100 μm, while, in a 10-mm sample, the resolution will be about 10 μm [262]. X-ray detectors have three main drawbacks.

1) X-ray imaging detects not only metals but also other nonmetallic materials (depending on their density and mass number) such as bone or stone. Thus, in order to detect only metallic particles and to distinguish different metals, the device has to be coupled to a chemical inspection element such as in [266].
2) The X-ray method is costly and requires high voltage power supplies [276].
3) X-rays can sometimes cause ionization and, thus, damage the sample, e.g., when applied in food, X-rays can damage some bacteria and degrade food taste [98]; however, soft X-rays have been used for the detection of metals in food inspection [263]. Thus, the effect of X-rays on a freeze-dried vaccine should be analyzed.

The sample analysis can be complemented with the reconstruction of a surface profile, which can be done with optical light using coherence scanning interferometry (CSI) [73] and digital shearography [277], both providing rapid measurements; however, metal particles cannot be distinguished from nonmetal particles.

3) Spectroscopic Analysis Techniques: The light absorbed or emitted by the sample can be used for deducing the elemental and chemical composition through spectrometric analysis. This can be performed using: 1) visible, ultraviolet (UV) light, and X-rays that interact with the electrons in the atoms yielding elemental information and 2) IR and near-IR light that interact with molecular bonds yielding molecular information.

Using visible light, atomic absorption spectroscopy (AAS) and atomic emission spectroscopy (AES) have been used for providing the elemental composition of aqueous solutions [278] and performing oil analysis [279], [280], [281], [282], [283], [284], [285], allowing the detection of metal particles [286], [287], [288], [289], [290]. However, these two methods require the atomization of the sample since the atoms have to be in their ground state in order to allow the atomic absorption to occur [291]. A variant of AES, laser-induced breakdown spectroscopy (LIBS), provides an in situ quantitative and qualitative analyses of samples and has been used for detecting metals in food [292], [293], [294], semiconductor manufacturing [295], oil [296], [297], and so on [236], [296], [298], [299], [300], [301], [302], [303], [304], [305], [306], [307], [308], [309]. However, it employs a pulsed high energy laser focused on a part of the sample, inducing high-temperature plasma and, thus, exciting the atoms of the sample, resulting in a small part of the sample being ablated. In addition, it only provides a near-surface analysis.

In laser-induced fluorescence (LIF), visible or UV light is sent to the sample, and the fluorescent radiation is collected and used for sensing the elemental composition. LIF allows the detection of elements with excellent sensitivity since the signal is observed against a dark background [310]. It is nonintrusive and nondestructive, and requires little to no sample preparation [311]. In addition, 2-D and 3-D images can be obtained [310] with a resolution below the mm range [312]. LIF imaging has been applied in aqueous flows [313] and combustions of propellants [314], [315] detecting iron atoms [314] and aluminum atoms [315]; however, we contend that the low penetration of visible and UV radiation in an opaque sample would prevent its use on vaccines.

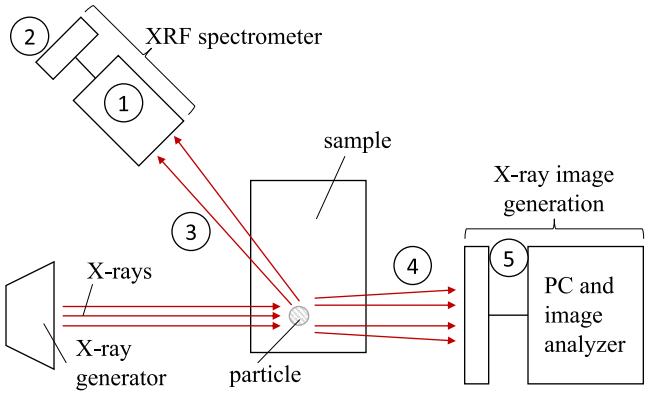

Fig. 5. Schematic of X-ray methods that rely on imaging and XRF. The main components of the setup are ① collimating/focusing assembly, ② X-ray detector (such as a silicon drift detector) for elemental analysis, ③ X-rays emitted by the sample, ④ transmitted/forward-scattered X-rays, and ⑤ X-ray detector for image generation (such as a super metal intensifier camera [263]). Adapted from [263] and [316].

The use of X-rays, with a higher penetration depth than visible and UV light, allows the analysis of particles at deeper locations in the sample. In X-ray fluorescence (XRF), the sample is excited with X-rays, and the secondary (fluorescent) X-rays emitted by its atoms are detected and used to obtain the quantitative elemental composition. XRF is simple, rapid, and nondestructive, and the analysis is not limited by the size of the particles, contrary to AAS or AES [317]. XRF has been used for detecting metal particles in lubricating oil [106], [318] and to estimate metal particle concentration [317], [319] for concentrations down to 1 ppm such as iron [319] and copper [318]. Furthermore, XRF can be used for performing inline and real-time analysis of a moving sample [316], and with a similar working principle, it could be used for inline vaccine inspection. In addition, XRF can be used in combination with X-ray imaging for obtaining both an image and elemental information [266]. Fig. 5 provides a schematic of the working principle of the inline XRF approach [316] and the X-ray transmission imaging approach [263]. Note that the ionization effects on a vaccine due to the exposition to X-rays should be studied. The sample can also be excited with beams of accelerated electrons in order to detect the emitted X-rays; however, this approach would harm the sample and can only give information about the near-surface. In order to achieve a more complete analysis, X-ray absorption spectroscopy (XAS) can also be used, providing electronic information, local structures of the sample, and average diameter of particles [320]; it has been previously

TABLE III
SUMMARY OF THE MAIN METHODS THAT CAN BE USED FOR DETECTING METAL PARTICLES IN FREEZE-DRIED VACCINES

Method	Advantages	Disadvantages/Need for Future Work
X-rays	Detects materials with relatively high atomic number and/or high density (e.g. metal, stone, bone). High penetration, rapid, high resolution, used in food control. Provides elemental composition when coupled with XRF (non-destructive). 3D information with XCT.	Danger of X-rays and possible ionization of vaccine. (Study of X-ray effects on vaccine is required.) Difficult to detect small particles ($\lesssim 300\ \mu$m) and aluminum. Ambiguity between metal & other high density particles. Higher resolution results in greater run times, resolution decreases in larger samples. Expensive and requires high voltage power.
Thermal imaging	Detects metal particles in a non-conductive medium. Non-contact.	Requires testing with metal particles inside a vaccine. Metal particles can heat and denature the vaccine. Heat measurements are affected by packaging surfaces [242].
Hyperspectral imaging	Provides image and chemical information. Non-ionizing and non-invasive.	Limited penetration of IR/NIR. Future work expected on the penetration of IR/NIR in a freeze-dried vaccine. No tests with metallic microparticles. Requires long time for data processing [242], [254].
THz	Easy distinction of conductive particles in a non-conductive medium [223]. Non-ionizing, non-invasive, spectral fingerprinting [222], high penetration in non-conductive and nonpolar materials. Higher contrast than X-rays [29].	Water strongly reflects THz. Sensibility can decrease in thicker samples. Resolution in the order of some hundred microns [243]. Future work expected on the use of quantum cascade laser with scanning mirror [248] for high-sensitivity and rapid inspection of a freeze-dried vaccine. Image processing algorithms will enable faster inspection.
SQUID-based detector	The most sensitive sensor to magnetic fields. High sensibility for ferrous particles while keeping relatively large particle-sensor distance. High sensibility in relatively wide areas using a multiple-sensor system [188].	Requires ultra-low temperatures, making application in industrial environments difficult. No reported tests with non-ferrous metal microparticles.
GMR/ TMR-based detector	High sensibility for ferrous particles. Low power, no need of ultra-low temperatures. Simple structure (GMR). TMR more sensible than GMR.	Large noise and complicated fabrication (TMR) [45]. No reported tests with non-ferrous metal microparticles.
RF inductive method	Detects all metal particles, distinguishes ferrous from non-ferrous particles, contactless, non-harmful, simple structure, rapid. Insensitive to air bubbles and non-metallic particles. Low influence under temperature and vibration. High penetration of RF waves.	Commercialized sensors can only detect ferrous particles $\gtrsim 100\ \mu$m and non-ferrous $\gtrsim 400\ \mu$m. Ferrous and non-ferrous particles passing simultaneously can be undetected.
RFID-based sensor	Fast, simple structure, high sensitivity while keeping high throughput. Not affected by air bubbles. High penetration of electric fields.	Cannot distinguish ferrous from non-ferrous metals. Future research required for noise reduction.
Capacitive sensor	Detects conductive particles in a non-conductive medium [84], fast, simple structure. High penetration of electric fields.	Ferrous & non-ferrous particles are indistinguishable. Air bubbles can cause false alarms. Signal depends on the chemical properties of the sample. Should study if electric fields affect the state of the vaccines.
Ultrasonic method	Can detect density changes, simple structure, with scanning acoustic tomography an image can be obtained, fast and non-destructive. Allows contactless inspection.	Temperature, sample viscosity, flow speed and mechanical vibration strongly affect its performance. Air highly attenuates the signal. Lower sensibility in non-homogeneous samples, limiting the detection depth. Requires studying the difference of the acoustic properties (e.g. absorption, reflection of acoustic waves) between the freeze-dried vaccine cake and the metal particles.

used for detecting small metal particles [320], [321], [322]. XRD provides information about the crystal structure and is nondestructive. It has been used for detecting and analyzing metal particles [323], [324] with sizes down to 1 nm using silicon slit detectors [324], measuring particle size [325]. However, only information about the near-surface is obtained, and it requires a prior preparation of the sample, which can be time-consuming and inefficient [224].

Molecular information can be obtained using IR spectroscopy (IRS) and Raman spectroscopy. IR rays interact with vibrating atomic bonds in the material, transferring molecules to higher energy states [326] at frequencies that depend on the elements involved in the bond and the molecular structure surrounding it [327]. Both IR spectroscopy and Raman spectroscopy are nondestructive and nonintrusive. IRS can detect metallic ions or atoms due to their interaction with the sample (such as the generation of new bonds and the interaction with functional groups) altering the IR spectrum [328], [329], [330]. IRS has been used for detecting metals in oil [329], in solutions even under relatively severe pressure and temperature conditions [331], in plants and soil [330], and in powders using diffuse reflectance IR Fourier transform spectroscopy (DRIFTS) [332]. However, in the transmission mode, solid samples have to be thinner than 20 μm [326] and sufficiently transparent to IR rays. For DRIFTS, the powder needs to be in direct contact with the IR light, and thus, its use on vaccines confined in glass tubes would make the detection more complex. Raman spectroscopy relies on the inelastic scattering of light. To produce a detectable signal surface, surface-enhanced Raman spectroscopy (SERS) is commonly used, where the sample is placed on a roughened metal surface, and a laser with light typically in the visible or near-IR range

is used [46]. SERS has been used for detecting metal ions [46], [333], [334]. However, the quality of the spectra might be affected by interference from the emitted fluorescence [29]. In addition, for near-IR and Raman spectroscopy/imaging, the penetration depth is in general lower than a few mm [245], making these methods inefficient for the inspection of an entire freeze-dried vaccine.

4) Ferrography: In the area of oil analysis, ferrography has been used for many years [37], [335], [336]. It relies on the use of magnets to accumulate ferrous particles on a glass slide, followed by an online analysis [35], [42], [337], [338], [339], [340] or an offline analysis after extraction of the substrate. However, its working principle makes it inapplicable in the inspection of vaccines.

E. Electron-Based Methods

Metal detection methods based on detecting electrons are mainly X-ray photoelectron spectroscopy (XPS) [322], [341], [342], [343] and electron microscopes [332], [344], [345], [346], [347], [348], [349], [350], [351], [352], [353], [354], [355]. In XPS, X-rays are sent through the sample and eject electrons from its atoms, yielding chemical information. However, only electrons from a depth of a few nanometers can be detected [342], and the method can only be applied in solids or powders and requires high vacuum [341], [342]. In electron microscopes, beams of accelerated electrons are sent to the sample, and the scattered and transmitted electrons are detected. However, the transmission electron microscope can only be applied in ultrathin samples, with a thickness of only a few hundreds of nanometers [356], such that electrons can pass through the specimen. The scanning electron microscope only provides information from a depth of up to a few micrometers [346]. In addition, the electron beam can damage the sample.

VI. Satisfaction of Vaccine Inspection Requirements

The vaccine inspection methods must satisfy the requirements listed in Table II. However, there is currently no single method fulfilling all the criteria, as we summarize in Table III. Instead of evaluating each reviewed method's partial fulfillment of Table II, we focus, in this section, on the most promising combination of techniques for vaccine analysis. This promising set comprises soft X-ray detection, THz imaging, and magnetic detectors—represented in the abstract figure—which can be integrated inline using a noncontact approach. Each of these methods exhibits the potential of detecting stainless steel particles in vaccines. In addition, inductive sensors are insensitive to nonmetal particles, X-ray detectors to low-density debris, and THz sensors to nonconductive particulates. Hence, their simultaneous use can lead to the specific distinction of stainless steel contaminants.

In terms of nondestructiveness, magnetic and THz methods fulfill the requirement. Although X-rays have the potential to ionize and harm the vaccine cake, soft X-rays have been used in food inspection in a nonharmful way. Therefore, the application of soft X-rays in vaccine analysis should be investigated.

Regarding speed, X-ray detectors can be used on conveyor belts at speeds of 80 m/min, and commercialized inductive detectors reach speeds of 12 L/min in oil channels, which indicates that both approaches may meet the speed requirement of Table II. However, for THz inspection, the detection times can vary depending on the setup used; for instance, if the laser is scanned over the sample surface, it may lead to detection times below the expected speed. Further testing is necessary to determine the applicability of THz methods in vaccine inspection.

TABLE IV
Order of Magnitude Estimates for Minimum Detectable Particle Sizes for Acceptable Detection Methods

Method	Minimum detectable size
Thermal camera	100 μm
THz imaging	100 μm
Resisitive capacitive sensors	10 μm
Inductive sensors	1 μm
RFID-based sensors	1 μm
Ultrasonic sensors	1 μm
Scanning acoustic sensor	1 μm
THz scatter method	100 nm
Magnetoresistive sensors (AMR, GMR, TMR)	10 nm
SQUID sensors	10 nm
Hall effect sensors	10 nm

Table IV outlines the order of magnitude estimates of the minimum detectable particle size for each method identified as acceptable for freeze-dried vaccine inspection. Commercialized inductive sensors can detect ferrous particles roughly above 60 μm in diameter in nonconductive samples, and detection below that limit is mostly conditioned by factors such as noise and particle-sensor distance. However, we believe the integration of high-sensibility magnetic sensors such as SQUIDs or GMR/TMR sensors, and the development of new coil structures adapted to vaccine vials can lead to an increase in the detectable particle size. Commercialized X-ray detectors can detect 0.3-mm metal particles, and in planar samples, 20-μm particles can be detected; however, the detectable size inside the vaccine cake remains unclear, as it depends on factors such as the absorption of the X-rays by the vaccine cake. Similarly, the detection capabilities with THz depend on the absorption properties of the vaccine cake, and thus, we expect experiments to know the size detection limits with both X-rays and THz. It is also important to note that, either using magnetic, X-ray, or THz detectors, the signal caused by many small particles may be interpreted as a single larger particle. Therefore, these sensors must incorporate an automatic analysis of the signals.

Finally, the detection capability of these techniques for stainless steel particles at any potential vaccine locations remains unclear. To resolve this uncertainty, further experiments in this area are expected.

VII. Conclusion and Future Work

We have conducted what we believe to be the first comprehensive review of metal detection methods, covering more methods than former reviews. Based on our research, we conclude that detecting metal particles in freeze-dried vaccines is indeed possible under current manufacturing

requirements. The main methods that we propose to explore for detecting metal particles in freeze-dried vaccines are summarized in Table III. In particular, we find RFID-based sensors, magnetic detectors based on inductive, SQUID, and GMR/TMR sensors, THz imaging, hyperspectral imaging, thermal imaging, and X-ray inspection to be promising approaches. Table IV summarizes the limitations of these methods in terms of the order of magnitude of the minimum particle size that may be detected using the method. For some methods, the minimum detectable sizes were demonstrated in experiments that sought to detect clusters of multiple particles due to the nature of the investigated application. In reality, the minimum detectable size for a single particle might, therefore, be larger for these methods.

Despite limited experiments on vaccines, we believe that most of the reported detection techniques could be used without—or with slight—modifications to test for detection reliability in vaccines.

Some material properties of freeze-dried vaccines may limit the detection methods. These material characteristics encompass a range of factors, including the magnitude of the acoustic reflection coefficient, electrical conductivity, dielectric permittivity, magnetic permeability, the depth to which static electric or magnetic fields penetrate the material, and the skin depth of various electromagnetic waves, e.g., RF, THz, IR, visible light, UV, and X-rays. Additionally, consideration should be given to whether there are notable ionization effects resulting from brief exposure to UV and X-rays. However, these material properties are unknown for freeze-dried vaccines and should be studied in the future to address their impact. The glass container of vaccines could further affect metal particle detection. For example, the glass container may distort light beams and cause measurement errors.

The one dimension that remains to be established for most detection techniques is detection depth as a function of particle size in vaccine samples. This would establish the minimum detectable particle size as a function of depth for each method. Depth detection graphs will allow a better evaluation and comparison of the performance of different techniques. Another metric that needs to be established in the future is the speed of inspection for each detection method, which we believe will be a function of the size and material of the sample.

Finally, physical effects, such as the coupling effect of multiple particles in the generation of electromagnetic signals, are not yet fully understood and can lead to detection errors. Future research is required to explore such effects through testing or simulation.

While this analysis focuses on the detection of stainless steel particles in vaccine vials due to stainless steel being the most common material in vaccine production machines, other metal particles may possibly be present in vaccines as well. Particles of a metal other than stainless steel are the subject of a future analysis.

REFERENCES

[1] Z. Ghaemmaghamian, R. Zarghami, G. Walker, E. O'Reilly, and A. Ziaee, "Stabilizing vaccines via drying: Quality by design considerations," *Adv. Drug Del. Rev.*, vol. 187, Aug. 2022, Art. no. 114313.

[2] M. Cuddihy, A. Gennari, T. Holt, and C. O'Sullivan, "Building greater resilience in vaccine manufacturing," McKinsey Company, New York, NY, USA, Tech. Rep., 2022.

[3] K. A. McLean, S. Goldin, C. Nannei, E. Sparrow, and G. Torelli, "The 2015 global production capacity of seasonal and pandemic influenza vaccine," *Vaccine*, vol. 34, no. 45, pp. 5410–5413, Oct. 2016.

[4] *Global Vaccine Market Report 2022: A Shared Understanding for Equitable Access to Vaccines*, World Health Org., Geneva, Switzerland, 2023.

[5] G. Allison et al., "Regulatory and quality considerations for continuous manufacturing. May 20–21, 2014 continuous manufacturing symposium," *J. Pharmaceutical Sci.*, vol. 104, no. 3, pp. 803–812, 2015.

[6] S. Byrn et al., "Achieving continuous manufacturing for final dosage formation: Challenges and how to meet them. May 20–21, 2014 continuous manufacturing symposium," *J. Pharmaceutical Sci.*, vol. 104, no. 3, pp. 792–802, Mar. 2015.

[7] B. N. Thorat, A. Sett, and A. S. Mujumdar, "Drying of vaccines and biomolecules," *Drying Technol.*, vol. 40, no. 3, pp. 461–483, Feb. 2022.

[8] J. F. Carpenter, M. J. Pikal, B. S. Chang, and T. W. Randolph, "Rational design of stable lyophilized protein formulations: Some practical advice," *Pharmaceutical Res.*, vol. 14, no. 8, p. 969, 1997.

[9] S. Ohtake, K.-I. Izutsu, and D. Lechuga-Ballesteros, *Drying Technologies for Biotechnology and Pharmaceutical Applications*. Hoboken, NJ, USA: Wiley, 2020.

[10] Centers for Disease Control and Prevention, "Vaccine storage and handling toolkit," Atlanta, GA, USA, Tech. Rep., 2022.

[11] M. Pelliccia et al., "Additives for vaccine storage to improve thermal stability of adenoviruses from hours to months," *Nature Commun.*, vol. 7, no. 1, pp. 1–7, Nov. 2016.

[12] D. J. A. Crommelin, T. J. Anchordoquy, D. B. Volkin, W. Jiskoot, and E. Mastrobattista, "Addressing the cold reality of mRNA vaccine stability," *J. Pharmaceutical Sci.*, vol. 110, no. 3, pp. 997–1001, Mar. 2021.

[13] M. L. Fahrni et al., "Management of COVID-19 vaccines cold chain logistics: A scoping review," *J. Pharmaceutical Policy Pract.*, vol. 15, no. 1, pp. 1–14, Dec. 2022.

[14] Deutsche Post DHL Group, "Delivering pandemic resilience," Bonn, Germany, Tech. Rep., 2020.

[15] L. Hinnant and S. Mednick, "Vaccine storage issues could leave 3B people without access," Associated Press, New York, NY, USA, 2020.

[16] M. R. Toler and S. Nema, "Visual inspection," in *Parenteral Medications*. Boca Raton, FL, USA: CRC Press, 2019, pp. 863–878.

[17] A. Flaquiere and J. Malthete, "Qualification of manual visual inspection still critical," Parenteral Drug Assoc., Bethesda Towers, MD, USA, 2020.

[18] J. D. Ayres, "Conducting clinical risk assessments for visible particulate matter in parenteral preparations," *PDA J. Pharmaceutical Sci. Technol.*, vol. 72, no. 6, pp. 626–639, 2018.

[19] R. Swift, "Japan's takeda says 'human error' caused contamination of moderna vaccines," Thomson Reuters, Los Angeles, CA, USA, 2021.

[20] H. Shibata et al., "Investigation of foreign particles in moderna COVID-19 vaccine," *Yakugaku Zasshi, J. Pharmaceutical Soc. Japan*, vol. 142, no. 8, pp. 867–874, 2022.

[21] E. Freund, "Appearance evaluation of parenteral pharmaceutical products," in *Sterile Product Development*. New York, NY, USA: Springer, 2013, pp. 411–430.

[22] P. Sharan, D. Tellbach, and S. E. Sarma, "Using edge detection and polarimetric imaging for vaccine inspection," *Proc. SPIE*, vol. 12046, pp. 93–107, Apr. 2022.

[23] M. Zhao, H. Zhang, L. Liu, Z. Liang, and G. Deng, "Joint deep learning and clustering algorithm for liquid particle detection of pharmaceutical injection," in *Proc. 8th Int. Conf. Image Process. Theory, Tools Appl. (IPTA)*, Nov. 2018, pp. 1–6.

[24] H. Zhang et al., "Automated machine vision system for liquid particle inspection of pharmaceutical injection," *IEEE Trans. Instrum. Meas.*, vol. 67, no. 6, pp. 1278–1297, Jun. 2018.

[25] C. Tsay and Z. Li, "Automating visual inspection of lyophilized drug products with multi-input deep neural networks," in *Proc. IEEE 15th Int. Conf. Autom. Sci. Eng. (CASE)*, Aug. 2019, pp. 1802–1807.

[26] G. Palmer, B. Schnieders, R. Savani, K. Tuyls, J.-D. Fossel, and H. Flore, "The automated inspection of opaque liquid vaccines," 2020, *arXiv:2002.09406*.

[27] Y. Zheng et al., "Determination of moisture content of lyophilized allergen vaccines by NIR spectroscopy," *J. Pharmaceutical Biomed. Anal.*, vol. 46, no. 3, pp. 592–596, 2008.

[28] K. T. Briggs, M. B. Taraban, and Y. B. Yu, "Quality assurance at the point-of-care: Noninvasively detecting vaccine freezing variability using water proton NMR," *Vaccine*, vol. 38, no. 31, pp. 4853–4860, Jun. 2020.

[29] I. E. Achouri, A. Rhoden, S. Hudon, R. Gosselin, J.-S. Simard, and N. Abatzoglou, "Non-invasive detection technologies of solid foreign matter and their applications to lyophilized pharmaceutical products: A review," *Talanta*, vol. 224, Mar. 2021, Art. no. 121885.

[30] J. C. May, T. C. Rains, F. J. Maienthal, G. N. Biddle, and J. J. Progar, "A survey of the concentrations of eleven metals in vaccines, allergenic extracts, toxoids, blood, blood derivatives and other biological products," *J. Biol. Standardization*, vol. 14, no. 4, pp. 363–375, Jan. 1986.

[31] R. Jia, L. Wang, C. Zheng, and T. Chen, "Online wear particle detection sensors for wear monitoring of mechanical equipment—A review," *IEEE Sensors J.*, vol. 22, no. 4, pp. 2930–2947, 2022.

[32] W. Hong, W. Cai, S. Wang, and M. M. Tomovic, "Mechanical wear debris feature, detection, and diagnosis: A review," *Chin. J. Aeronaut.*, vol. 31, no. 5, pp. 867–882, May 2018.

[33] J. Sun, L. Wang, J. Li, F. Li, J. Li, and H. Lu, "Online oil debris monitoring of rotating machinery: A detailed review of more than three decades," *Mech. Syst. Signal Process.*, vol. 149, Feb. 2021, Art. no. 107341.

[34] S. Yang, N. Cao, and B. Yu, "Wear debris measurement in lubricating oil based on inductive method: A review," *Meas. Control*, vol. 56, nos. 7–8, pp. 1422–1435, Sep./Oct. 2023.

[35] N. K. Myshkin and L. V. Markova, "Wear prediction for tribosystems based on debris analysis," in *On-Line Condition Monitoring in Industrial Lubrication and Tribology*. Springer, 2018, pp. 131–201.

[36] S. Murali, A. V. Jagtiani, X. Xia, J. Carletta, and J. Zhe, "A microfluidic Coulter counting device for metal wear detection in lubrication oil," *Rev. Sci. Instrum.*, vol. 80, no. 1, Jan. 2009, Art. no. 016105.

[37] M. Lukas and D. Anderson, "Lubricant analysis for gas turbine condition monitoring," in *Proc. Turbo Expo, Power Land, Sea, Air*, vol. 78774, 1996, Art. no. V001T09A001.

[38] E. Trumsina, S. Kukle, and G. Zommere, "Nano scale methods for water pollution monitoring," in *Proc. Int. Sci. Practical Conf.*, vol. 1, 2011, pp. 97–103.

[39] I. Cretescu, M. D. Tutulea, D. Sibiescu, and C. Stan, "Electrochemical sensors for heavy metal ions detection from aqueous solutions," *Environ. Eng. Manage. J.*, vol. 11, no. 2, pp. 463–470, 2012.

[40] A. Davis, *Handbook of Condition Monitoring*. London, U.K.: Chapman & Hall, 1988.

[41] B. Rao, *Handbook of Condition Monitoring*. Amsterdam, The Netherlands: Elsevier, 1996.

[42] T. M. Hunt, *Handbook of Wear Debris Analysis and Particle Detection in Liquids*. Barking, U.K.: Elsevier, 1993.

[43] G. R. Humphrey and R. W. Martin, *1998 Technology Showcase. JOAP International Condition Monitoring Conference*. Pensacola, FL, USA: Technical Support Center, Joint Oil Analysis Program, Apr. 1998.

[44] A. Davies, *Handbook of Condition Monitoring: Techniques and Methodology*. Dordrecht, The Netherlands: Springer, 2012.

[45] R. Abedini-Nassab, M. P. Miandoab, and M. Şaşmaz, "Microfluidic synthesis, control, and sensing of magnetic nanoparticles: A review," *Micromachines*, vol. 12, no. 7, p. 768, 2021.

[46] G. Xu, P. Song, and L. Xia, "Examples in the detection of heavy metal ions based on surface-enhanced Raman scattering spectroscopy," *Nanophotonics*, vol. 10, no. 18, pp. 4419–4445, Dec. 2021.

[47] US Pharmacopeial Convention, "General chapter <790> visible particulates in injections," USP, Rockville, MD, USA, Tech. Rep. USP 42–NF 37, 2019, p. 6947

[48] "Chapter 2.9.20 particulate contamination: Visible particles," 8th ed., Eur. Pharmacopeia, Strasbourg, France, 2013.

[49] "Chapter 6.06, foreign matter test for injections," 16th ed., Jpn. Pharmacopeia, Tokyo, Japan, 2011.

[50] "General chapter <788> particulate matter in injections," U.S. Pharmacopeia, North Bethesda, MD, USA, Tech. Rep. USP 34, 2011.

[51] J. Z. Knapp and H. K. Kushner, "Implementation and automation of a particle detection system for parenteral products," *PDA J. Pharmaceutical Sci. Technol.*, vol. 34, no. 5, pp. 369–393, 1980.

[52] A. Zaffora, F. Di Franco, and M. Santamaria, "Corrosion of stainless steel in food and pharmaceutical industry," *Current Opinion Electrochemistry*, vol. 29, Oct. 2021, Art. no. 100760.

[53] A. L. Gray et al., *Applications of Inductively Coupled Plasma Mass Spectrometry*. Vienna, Austria: International Atomic Energy Agency (IAEA), 1989.

[54] B. Sampson and A. Hart, "Clinical usefulness of blood metal measurements to assess the failure of metal-on-metal hip implants," *Ann. Clin. Biochemistry, Int. J. Lab. Med.*, vol. 49, no. 2, pp. 118–131, Mar. 2012.

[55] P. T. Nilsson et al., "Nano-objects emitted during maintenance of common particle generators: Direct chemical characterization with aerosol mass spectrometry and implications for risk assessments," *J. Nanoparticle Res.*, vol. 15, no. 11, pp. 1–16, Nov. 2013.

[56] C. P. Lee, "Novel mass spectrometry technique developments for a more holistic characterization of atmospheric constituents: More molecular detection with quantification capability," Ph.D. thesis, Dept. Chem. Appl. Biosci., ETH Zürich, Zürich, Switzerland, 2021.

[57] Y. Qu, H. Ji, F. Oudray, Y. Yan, and Y. Liu, "Online composition detection and cluster analysis of Tibetan incense," *Optik*, vol. 241, Sep. 2021, Art. no. 166999.

[58] S. Giannoukos et al., "Detection of trace metals in biogas using extractive electrospray ionization high-resolution mass spectrometry," *Renew. Energy*, vol. 169, pp. 780–787, May 2021.

[59] K. Chana, "Practical on and off-wing applications of a thermal product measurement sensor for detection of contamination in fluids," NATO, Brussel, Belgium, Tech. Rep. STO-MP-AVT-306.

[60] L. C. Maier Jr., and J. C. Slater, "Field strength measurements in resonant cavities," *J. Appl. Phys.*, vol. 23, no. 1, pp. 68–77, Jan. 1952.

[61] M. Ikeda, M. Ignatenko, A. Mase, and K. Uchino, "Modeling and experimental detection of resonance frequency shift of a microwave cavity caused by a small conductive particle," *J. Electromagn. Waves Appl.*, vol. 27, no. 9, pp. 1114–1126, 2013.

[62] M. Ikeda, A. Mase, and K. Uchino, "Small conductive particle detection with a microwave resonant cavity," *Electr. Eng. Jpn.*, vol. 186, no. 2, pp. 61–67, Jan. 2014.

[63] N. K. Myshkin and L. V. Markova, "Wear prediction for tribosystems basedon debris analysis," in *On-Line Condition Monitoring in Industrial Lubrication and Tribology*. Springer, 2018, pp. 131–201.

[64] J. Edmonds, M. S. Resner, and K. Shkarlet, "Detection of precursor wear debris in lubrication systems," in *Proc. IEEE Aerosp. Conf.*, vol. 6, Mar. 2000, pp. 73–77.

[65] M. A. Sarangi, "Oil debris detection using capacitance and ultrasonic measurements," Ph.D. thesis, Dept. Mech. Eng., Univ. Akron, Akron, OH, USA, 2007.

[66] C. P. Nemarich, H. K. Whitesel, and A. Sarkady, "On-line wear-particle monitoring based on ultrasonic detection and discrimination," *Mater. Eval. (USA)*, vol. 50, no. 4, pp. 525–530, 1988.

[67] L. Du and J. Zhe, "An integrated ultrasonic–inductive pulse sensor for wear debris detection," *Smart Mater. Struct.*, vol. 22, no. 2, Feb. 2013, Art. no. 025003.

[68] C. Xu, P. Zhang, H. Wang, Y. Li, and C. Lv, "Ultrasonic echo waveshape features extraction based on QPSO-matching pursuit for online wear debris discrimination," *Mech. Syst. Signal Process.*, vols. 60–61, pp. 301–315, Aug. 2015.

[69] Y. Li and P. Zhang, "An online de-noising method for oil ultrasonic wear debris signal: Fuzzy morphology component analysis," *Ind. Lubrication Tribol.*, vol. 70, no. 6, pp. 1012–1019, 2018.

[70] G. Ansley, S. Bakanas, M. Castronuovo, T. Grant, and F. Vichi, "Current nondestructive inspection methods for aging aircraft," Galaxy Sci. Corp., Mays Landing, NJ, USA, FAA Rep. DOT/FAA/CT-91/5, 1992.

[71] E. Hæggström and M. Luukkala, "Ultrasound detection and identification of foreign bodies in food products," *Food Control*, vol. 12, no. 1, pp. 37–45, Jan. 2001.

[72] B. Zhao, O. A. Basir, and G. S. Mittal, "Detection of metal, glass and plastic pieces in bottled beverages using ultrasound," *Food Res. Int.*, vol. 36, no. 5, pp. 513–521, Jan. 2003.

[73] R. Tamochi, S. Ito, K. Hayakawa, and T. Masuda, "Hitachi's measurement and analysis technologies for future science and social innovation," *Hitachi Rev.*, vol. 65, no. 7, p. 177, 2016.

[74] M. T. M. Khairi, S. Ibrahim, M. A. M. Yunus, and M. Faramarzi, "Contact and non-contact ultrasonic measurement in the food industry: A review," *Meas. Sci. Technol.*, vol. 27, no. 1, Jan. 2016, Art. no. 012001.

[75] B.-K. Cho and J. M. K. Irudayaraj, "Foreign object and internal disorder detection in food materials using noncontact ultrasound imaging," *J. Food Sci.*, vol. 68, no. 3, pp. 967–974, Apr. 2003.

[76] D. L. Naas, "Metal particle detector apparatus for non-conducting fluid systems," U.S. Patent 5 402 113, Mar. 28, 1995.

[77] H. Powrie, C. Fisher, O. Tasbaz, and R. Wood, "Performance of an electrostatic oil monitoring system during an FZG gear scuffing test," in *Proc. Int. Conf. Condition Monitor.*, Oxford, U.K.: Coxmore Publishing, 1999, pp. 145–155.

[78] X. Tang, Z. Chen, Y. Li, and Y. Yang, "Compressive sensing-based electrostatic sensor array signal processing and exhausted abnormal debris detecting," *Mech. Syst. Signal Process.*, vol. 105, pp. 404–426, May 2018.

[79] Z. Jin and F. Zhang, "Analysis of spatial sensitivity based on electrostatic monitoring technique in oil-lubricated system," *Open Access Library J.*, vol. 5, no. 10, pp. 1–13, 2018.

[80] X. Tang, Z.-S. Chen, Y. Li, Z. Hu, and Y.-M. Yang, "Analysis of the dynamic sensitivity of hemisphere-shaped electrostatic Sensors' circular array for charged particle monitoring," *Sensors*, vol. 16, no. 9, p. 1403, Aug. 2016.

[81] H. Mao, H. Zuo, H. Wang, Y. Yin, and X. Li, "Debris recognition methods in the lubrication system with electrostatic sensors," *Math. Problems Eng.*, vol. 2018, pp. 1–15, Dec. 2018.

[82] E. C. Gregg and K. D. Steidley, "Electrical counting and sizing of mammalian cells in suspension," *Biophysical J.*, vol. 5, no. 4, pp. 393–405, Jul. 1965.

[83] C. A. Megerle, "Oil quality monitor sensor and system," U.S. Patent 5 089 780, Feb. 18, 1992.

[84] X. Xia, "Modeling a microfluidic capacitive sensor for metal wear debris detection in lubrication oil," Ph.D. thesis, Dept. Elect. Eng., Univ. Akron, Akron, OH, USA, 2009.

[85] A. V. Jagtiani, "Novel multiplexed Coulter counters for high throughput parallel analysis of microparticles," Ph.D. thesis, Univ. Akron, 2011.

[86] L. Zeng, W. Wang, F. Rogers, H. Zhang, X. Zhang, and D. Yang, "A high sensitivity micro impedance sensor based on magnetic focusing for oil condition monitoring," *IEEE Sensors J.*, vol. 20, no. 7, pp. 3813–3821, Apr. 2020.

[87] T. Islam, M. Yousuf, and M. Nauman, "A highly precise cross-capacitive sensor for metal debris detection in insulating oil," *Rev. Sci. Instrum.*, vol. 91, no. 2, Feb. 2020, Art. no. 025005.

[88] H. Gao, Y. Min, and Q. Chang, "Metal particles velocity measurement based on capacitance sensor with double triangular-shaped electrodes," *IEEE Sensors J.*, vol. 22, no. 12, pp. 11827–11834, Jun. 2022.

[89] L. Zeng, Z. Yu, H. Zhang, X. Zhang, and H. Chen, "A high sensitive multi-parameter micro sensor for the detection of multi-contamination in hydraulic oil," *Sens. Actuators A, Phys.*, vol. 282, pp. 197–205, Oct. 2018.

[90] D. M. Dobkin and S. M. Weigand, "Environmental effects on RFID tag antennas," in *IEEE MTT-S Int. Microw. Symp. Dig.*, Jun. 2005, pp. 135–138.

[91] X. Qing and Z. N. Chen, "Proximity effects of metallic environments on high frequency RFID reader antenna: Study and applications," *IEEE Trans. Antennas Propag.*, vol. 55, no. 11, pp. 3105–3111, Nov. 2007.

[92] A. Yin and H. Ren, "Monitoring wear debris in oil utilizing rfid signal transmission features," *China Mech. Eng.*, vol. 26, no. 24, p. 3356, 2015.

[93] A. M. J. Marindra and G. Y. Tian, "Chipless RFID sensor tag for metal crack detection and characterization," *IEEE Trans. Microw. Theory Techn.*, vol. 66, no. 5, pp. 2452–2462, May 2018.

[94] J. Wang, X. Chen, K. Wu, M. Zhang, and W. Huang, "Highly-sensitive electrochemical sensor for Cd^{2+} and Pb^{2+} based on the synergistic enhancement of exfoliated graphene nanosheets and bismuth," *Electroanalysis*, vol. 28, no. 1, pp. 63–68, Jan. 2016.

[95] W. Xiong, L. Zhou, and S. Liu, "Development of gold-doped carbon foams as a sensitive electrochemical sensor for simultaneous determination of Pb (II) and Cu (II)," *Chem. Eng. J.*, vol. 284, pp. 650–656, Jan. 2016.

[96] D. Gokul, E. Catton, K. Y. Cheng, and M. Mathew, "Electrochemical biosensor to detect implant-derived metal ions: A mice model," *J. Bio-Tribo-Corrosion*, vol. 9, no. 2, p. 28, Jun. 2023.

[97] C. Ariño et al., "Electrochemical stripping analysis," *Nature Rev. Methods Primers*, vol. 2, no. 1, pp. 1–18, 2022.

[98] S. Tanaka, T. Ohtani, Y. Narita, Y. Hatsukade, and S. Suzuki, "Development of metallic contaminant detection system using RF high-tc SQUIDs for food inspection," *IEEE Trans. Appl. Supercond.*, vol. 25, no. 3, pp. 1–4, Jun. 2015.

[99] Z. Yunbo and G. Yuhai, "Research of the on-line system for detecting metal particles in oil," in *Proc. 13th IEEE Int. Conf. Electron. Meas. Instrum. (ICEMI)*, Oct. 2017, pp. 98–102.

[100] V. A. Zarenkov, D. V. Zarenkov, and V. I. Dikarev, "Metal detector," Russian Patent 2 189 616 C1, 2002.

[101] B. Liu and W. Zhou, "The research of metal detectors using in food industry," in *Proc. Int. Conf. Electron. Optoelectron.*, vol. 4, Jul. 2011, pp. V4-43–V4-45.

[102] V. P. Alexandrov and A. A. Skorobogatov, "Method for detecting metal particles in moveable fiber material," Russian Patent 2 545 495 C1, 2015.

[103] M. T. S. Balkrishna and S. Pardeshi, "Model design and simulation of automatic counting machine using proximity sensor," *JournalNX—Multidisciplinary Peer Reviewed J.*, 2018.

[104] I. M. Flanagan, "An electronic system for wear-debris condition monitoring," Ph.D. thesis, Fac. Sci., Univ. Edinburgh, Edinburgh, U.K., 1987.

[105] L. Du, J. Carletta, R. Veillette, and J. Zhe, "A magnetic coulter counting device for wear debris detection in lubrication," in *Proc. ASME Int. Mech. Eng. Congr. Expo.*, vol. 43857, 2009, pp. 649–653.

[106] C. Byington, C. Palmer, G. Argenna, and N. Mackos, "An integrated, real-time oil quality monitor and debris measurement capability for drive train and engine systems," presented at the Amer. Helicopter Soc. 66th Annu. Forum, May 2010, pp. 11–13.

[107] L. Du, J. Zhe, J. E. Carletta, and R. J. Veillette, "Inductive Coulter counting: Detection and differentiation of metal wear particles in lubricant," *Smart Mater. Struct.*, vol. 19, no. 5, May 2010, Art. no. 057001.

[108] L. Du, J. Zhe, J. Carletta, R. Veillette, and F. Choy, "Real-time monitoring of wear debris in lubrication oil using a microfluidic inductive Coulter counting device," *Microfluidics Nanofluidics*, vol. 9, no. 6, pp. 1241–1245, Dec. 2010.

[109] D. Li, C. Joan, R. Veillette, and Z. Jiang, "An inductive Coulter counting device for online monitoring of wear debris in lubricant," in *Earth and Space 2010: Engineering, Science, Construction, and Operations in Challenging Environments*. Reston, VA, USA: American Society of Civil Engineers, 2010, pp. 1538–1545.

[110] L. Du and J. Zhe, "A high throughput inductive pulse sensor for online oil debris monitoring," *Tribol. Int.*, vol. 44, no. 2, pp. 175–179, Feb. 2011.

[111] J. P. Davis, J. E. Carletta, R. J. Veillette, L. Du, and J. Zhe, "Instrumentation circuitry for an inductive wear debris sensor," in *Proc. 10th IEEE Int. NEWCAS Conf.*, Jun. 2012, pp. 501–504.

[112] L. Du, "A multichannel oil debris sensor for online health monitoring of rotating machinery," Ph.D. thesis, Univ. Akron, Akron, OH, USA, 2012.

[113] L. Du, X. Zhu, Y. Han, L. Zhao, and J. Zhe, "Improving sensitivity of an inductive pulse sensor for detection of metallic wear debris in lubricants using parallel LC resonance method," *Meas. Sci. Technol.*, vol. 24, no. 7, Jul. 2013, Art. no. 075106.

[114] H. Zhang, X. Zhang, Y. Zhang, L. Guo, and Y. Sun, "Design of the oil detection microfluidic chip," *Chin. J. Sci. Instrum.*, vol. 34, no. 4, pp. 762–767, 2013.

[115] X. Zhang, H. Zhang, Y. Sun, H. Chen, and Y. Zhang, "Research on the output characteristics of microfluidic inductive sensor," *J. Nanomaterials*, vol. 2014, pp. 1–7, Mar. 2014.

[116] C. Wang, X. Liu, and Z. Chen, "A new inductive sensor for online health monitoring of mechanical transmission systems," in *Proc. IEEE Magn. Conf. (INTERMAG)*, May 2015, p. 1.

[117] C. Wang, X. Liu, H. Liu, and Z. Chen, "A new oil debris sensor for online condition monitoring of wind turbine gearboxes," in *Proc. EWEA Annu. Event*. Brussels, Belgium: The European Wind Energy Association, 2015.

[118] C. Wang, X. Liu, and Z. Chen, "Probe improvement of inductive sensor for online health monitoring of mechanical transmission systems," *IEEE Trans. Magn.*, vol. 51, no. 11, pp. 1–4, Nov. 2015.

[119] X. M. Zhang, H. P. Zhang, Z. Bo, H. Q. Chen, and Y. Q. Sun, "Study on magnetization and detection the metal particle in harmonic magnetic field," *Key Eng. Mater.*, vol. 645, pp. 790–795, Jun. 2015.

[120] E. Liu, H. Zhang, Y. Wu, H. Fu, Y. Sun, and H. Chen, "Effect of oil velocity on sensitivity of micron metal particle detection by inductive sensor. opt," *Precis. Eng*, vol. 24, no. 3, pp. 533–539, 2016.

[121] B. Liu, Y. Su, J. Yang, and J. Zhe, "Research on the relationship between the materials of magnetic cores and sensitivity of the micro planar inductive sensor," *Recent Patents Mech. Eng.*, vol. 9, no. 2, pp. 162–167, May 2016.

[122] B. Liu, Y. Su, and J. Yang, "The simulation research on the detection of metal particles with micro planar transformer sensor," *Recent Patents Mech. Eng.*, vol. 9, no. 1, pp. 57–62, Feb. 2016.

[123] C. Wang, "Health monitoring and fault diagnostics of wind turbines," Aalborg Univ., Aalborg, Denmark, Tech. Rep., 2016.

[124] Y. Wu, H. Zhang, L. Zeng, H. Chen, and Y. Sun, "Determination of metal particles in oil using a microfluidic chip-based inductive sensor," *Instrum. Sci. Technol.*, vol. 44, no. 3, pp. 259–269, May 2016.

[125] Y. Wu and H. Zhang, "An approach to calculating metal particle detection in lubrication oil based on a micro inductive sensor," *Meas. Sci. Technol.*, vol. 28, no. 12, Dec. 2017, Art. no. 125101.

[126] Y. Wu and H. Zhang, "Research on the effect of relative movement on the output characteristic of inductive sensors," *Sens. Actuators A, Phys.*, vol. 267, pp. 485–490, Nov. 2017.

[127] Y. Wu, H. Zhang, Y. Sun, and H. Chen, "Research on the influence of velocity on the sensitivity of inductive sensor," *J. Eng. Res.*, vol. 5, no. 2, pp. 129–140, 2017.

[128] X. Zhu, L. Du, and J. Zhe, "A 3×3 wear debris sensor array for real time lubricant oil conditioning monitoring using synchronized sampling," *Mech. Syst. Signal Process.*, vol. 83, pp. 296–304, Jan. 2017.

[129] Y. J. Ren, G. F. Zhao, M. Qian, and Z. H. Feng, "A highly sensitive triple-coil inductive debris sensor based on an effective unbalance compensation circuit," *Meas. Sci. Technol.*, vol. 30, no. 1, Jan. 2019, Art. no. 015108.

[130] R. Sanga, V. S. Srinivasan, M. Sivaramakrishna, and G. Prabhakara Rao, "Deployment of an inductance-based quasi-digital sensor to detect metallic wear debris in lubricant oil of rotating machinery," *Meas. Sci. Technol.*, vol. 29, no. 7, Jul. 2018, Art. no. 075102.

[131] Y. Wu, "Detection of foreign particles in lubrication oil with a microfluidic chip," *Ind. Lubrication Tribol.*, vol. 70, no. 8, pp. 1381–1387, 2018.

[132] Y. Wu, H. Zhang, M. Wang, and H. Chen, "Differentiation of nonferrous metal particles in lubrication oil using an electrical conductivity measurement-based inductive sensor," *Rev. Sci. Instrum.*, vol. 89, no. 2, Feb. 2018, Art. no. 025002.

[133] Z. Yu, L. Zeng, H. Zhang, G. Yang, W. Wang, and W. Zhang, "Frequency characteristic of resonant micro fluidic chip for oil detection based on resistance parameter," *Micromachines*, vol. 9, no. 7, p. 344, Jul. 2018.

[134] L. Zeng, H. Zhang, Q. Wang, and X. Zhang, "Monitoring of nonferrous wear debris in hydraulic oil by detecting the equivalent resistance of inductive sensors," *Micromachines*, vol. 9, no. 3, p. 117, Mar. 2018.

[135] C. Bai, H. Zhang, L. Zeng, X. Zhao, and Z. Yu, "High-throughput sensor to detect hydraulic oil contamination based on microfluidics," *IEEE Sensors J.*, vol. 19, no. 19, pp. 8590–8596, Oct. 2019.

[136] L. Ma, H. Zhang, W. Qiao, X. Han, L. Zeng, and H. Shi, "Oil metal debris detection sensor using ferrite core and flat channel for sensitivity improvement and high throughput," *IEEE Sensors J.*, vol. 20, no. 13, pp. 7303–7309, Jul. 2020.

[137] L. Ma, Z. Xu, H. Zhang, W. Qiao, and H. Chen, "Multifunctional detection sensor and sensitivity improvement of a double solenoid coil sensor," *Micromachines*, vol. 10, no. 6, p. 377, Jun. 2019.

[138] Y. Wu and H. Zhang, "Solid particles, water drops and air bubbles detection in lubricating oil using microfluidic inductance and capacitance measurements," *J. Micromech. Microeng.*, vol. 29, no. 2, Feb. 2019, Art. no. 025011.

[139] X. Zhang, L. Zeng, H. Zhang, and S. Huang, "Magnetization model and detection mechanism of a microparticle in a harmonic magnetic field," *IEEE/ASME Trans. Mechatronics*, vol. 24, no. 4, pp. 1882–1892, Aug. 2019.

[140] C. Bai et al., "Design and parameter research of time-harmonic magnetic field sensor based on PDMS in microfluidic technology," *Polymers*, vol. 12, no. 9, p. 2022, Sep. 2020.

[141] C. Bai, H. Zhang, L. Zeng, X. Zhao, and L. Ma, "Inductive magnetic nanoparticle sensor based on microfluidic chip oil detection technology," *Micromachines*, vol. 11, no. 2, p. 183, Feb. 2020.

[142] S. Feng, L. Yang, B. Fan, R. Li, J. Luo, and J. Mao, "A ferromagnetic wear particle sensor based on a rotational symmetry high-gradient magnetostatic field," *IEEE Trans. Instrum. Meas.*, vol. 70, pp. 1–9, 2021.

[143] L. Ma, H. Shi, H. Zhang, G. Li, Y. Shen, and N. Zeng, "High-sensitivity distinguishing and detection method for wear debris in oil of marine machinery," *Ocean Eng.*, vol. 215, Nov. 2020, Art. no. 107452.

[144] M. Qian, Y. Ren, G. Zhao, and Z. Feng, "Ultrasensitive inductive debris sensor with a two-stage autoasymmetrical compensation circuit," *IEEE Trans. Ind. Electron.*, vol. 68, no. 9, pp. 8885–8893, Sep. 2021.

[145] H. Shi, H. Zhang, L. Ma, F. Rogers, X. Zhao, and L. Zeng, "An impedance debris sensor based on a high-gradient magnetic field for high sensitivity and high throughput," *IEEE Trans. Ind. Electron.*, vol. 68, no. 6, pp. 5376–5384, Jun. 2021.

[146] Y. Wu and C. Yang, "Ferromagnetic metal particle detection including calculation of particle magnetic permeability based on micro inductive sensor," *IEEE Sensors J.*, vol. 21, no. 1, pp. 447–454, Jan. 2021.

[147] Y. Li, C. Yu, B. Xue, H. Zhang, and X. Zhang, "A double lock-in amplifier circuit for complex domain signal detection of particles in oil," *IEEE Trans. Instrum. Meas.*, vol. 71, pp. 1–10, 2022.

[148] Z. Niu, K. Li, W. Bai, Y. Sun, Q. Gong, and Y. Han, "Design of inductive sensor system for wear particles in oil," *J. Mech. Eng.*, vol. 57, no. 12, pp. 126–135, 2021.

[149] J. Park, S.-J. Yoo, J.-S. Yoon, and Y.-J. Kim, "Inductive particle detection system for real-time monitoring of metals in airborne particles," *Sens. Actuators A, Phys.*, vol. 332, Dec. 2021, Art. no. 113153.

[150] Y. Wu, F. Wang, M. Zhao, B. Wang, and C. Yang, "A method for measurement of nonferrous particles sizes in lubricant oil independent of materials using inductive sensor," *IEEE Sensors J.*, vol. 21, no. 16, pp. 17723–17731, Aug. 2021.

[151] X. Wu et al., "A new inductive debris sensor based on dual-excitation coils and dual-sensing coils for online debris monitoring," *Sensors*, vol. 21, no. 22, p. 7556, Nov. 2021.

[152] S. Wu et al., "A novel multichannel inductive wear debris sensor based on time division multiplexing," *IEEE Sensors J.*, vol. 21, no. 9, pp. 11131–11139, May 2021.

[153] Y. Xie, H. Zhang, H. Shi, and Y. Zhang, "Frequency research of microfluidic wear debris detection chip based on inductive wheatstone bridge," in *Proc. IEEE 16th Int. Conf. Nano/Micro Engineered Mol. Syst. (NEMS)*, Apr. 2021, pp. 780–785.

[154] S. Y. Borovik, I. G.-D. Korshikov, and Y. N. Sekisov, "Method of operating division of oil flow rate when detecting—Origination of metal particles in diamond means gnostics of GTE friction units," Russian Patent 2 749 574 C1, 2021.

[155] S. Y. Borovik, O. A. Zayakin, P. E. Podlipnov, and Y. N. Sekisov, "Effect of the oil flow rate on the result of detecting the wear particles of friction pairs in the lubrication systems of power units," *Optoelectron., Instrum. Data Process.*, vol. 58, no. 4, pp. 349–357, Aug. 2022.

[156] H. Huang, S. He, X. Xie, W. Feng, H. Zhen, and H. Tao, "Research on the influence of inductive wear particle sensor coils on debris detection," *AIP Adv.*, vol. 12, no. 7, Jul. 2022, Art. no. 075204.

[157] Z. Liu et al., "The optimization of parallel resonance circuit for wear debris detection by adjusting capacitance," *Energies*, vol. 15, no. 19, p. 7318, Oct. 2022.

[158] C. Wang et al., "An oil multipollutant detection sensor with high sensitivity and high throughput," *IEEE Trans. Instrum. Meas.*, vol. 71, pp. 1–11, 2022.

[159] C. Wang et al., "Research on high sensitivity oil debris detection sensor using high magnetic permeability material and coil mutual inductance," *Sensors*, vol. 22, no. 5, p. 1833, Feb. 2022.

[160] X. Shen, Q. Han, Y. Wang, B. Wu, and R. Zhu, "Research on detection performance of four-coil inductive debris sensor," *IEEE Sensors J.*, vol. 23, no. 7, pp. 6717–6727, Apr. 2023.

[161] C. Wang et al., "A sensor containing high permeability material for mechanical wear particle detection," *Sens. Actuators A, Phys.*, vol. 349, Jan. 2023, Art. no. 114075.

[162] P. A. Varady, T. Vockensohn, K. Forßmann, A. Ziegler, and J.-M. Seitz, "Non-invasive degradation tracking of mg implants in humans: A measurement approach," *JOM*, vol. 72, no. 5, pp. 1845–1850, May 2020.

[163] T. Chady, M. Enokizono, T. Todaka, Y. Tsuchida, and T. Yasutake, "Identification of three-dimensional distribution of metal particles using electromagnetic tomography system," *J. Mater. Process. Technol.*, vol. 181, nos. 1–3, pp. 177–181, Jan. 2007.

[164] A. I. Suzdaltsev and V. A. Lobanova, "Method for detecting metal particles in moving material," Russian Patent 2 147 327 C1, 2000.

[165] R. Y.-W. Wang, "Bearing fault detection and oil debris monitoring by adaptive noise cancellation," Ph.D. thesis, Dept. Mech. Eng., Univ. Ottawa, Ottawa, ON, Canada, 2008.

[166] W. Yuan, G. Dong, K. S. Chin, and M. Hua, "Tribological assessment of sliding pairs under damped harmonic excitation loading based on online monitoring methods," *Tribol. Int.*, vol. 96, pp. 225–236, Apr. 2016.

[167] W. Shang, Y. Wang, M. Zhang, and D. Liu, "Oil metal particles detection algorithm based on wavelet transform," in *Proc. MATEC Web Conf.*, vol. 100, 2017, p. 2001.

[168] X. Zhu, C. Zhong, and J. Zhe, "A high sensitivity wear debris sensor using ferrite cores for online oil condition monitoring," *Meas. Sci. Technol.*, vol. 28, no. 7, Jul. 2017, Art. no. 075102.

[169] Y. J. Ren, W. Li, G. F. Zhao, and Z. H. Feng, "Inductive debris sensor using one energizing coil with multiple sensing coils for sensitivity improvement and high throughput," *Tribol. Int.*, vol. 128, pp. 96–103, Dec. 2018.

[170] V. Belopukhov et al., "Monitoring metal wear particles of friction pairs in the oil systems of gas turbine power plants," *Energies*, vol. 15, no. 13, p. 4896, Jul. 2022.

[171] S. Feng, L. Yang, G. Qiu, J. Luo, R. Li, and J. Mao, "An inductive debris sensor based on a high-gradient magnetic field," *IEEE Sensors J.*, vol. 19, no. 8, pp. 2879–2886, Apr. 2019.

[172] C. S. Saba, "Determination of metallic iron in wear debris using a wear particle analyzer," *Wear*, vol. 129, no. 1, pp. 143–158, Jan. 1989.

[173] S. Showalter, S. Pingalkar, and S. Pasha, "Oil debris monitoring in aerospace engines and helicopter transmissions," in *Proc. 1st Int. Symp. Phys. Technol. Sensors (ISPTS)*, Mar. 2012, pp. 157–160.

[174] W. Hong, S. Wang, M. M. Tomovic, H. Liu, and X. Wang, "A new debris sensor based on dual excitation sources for online debris monitoring," *Meas. Sci. Technol.*, vol. 26, no. 9, Sep. 2015, Art. no. 095101.

[175] H. Xiao, X. Wang, H. Li, J. Luo, and S. Feng, "An inductive debris sensor for a large-diameter lubricating oil circuit based on a high-gradient magnetic field," *Appl. Sci.*, vol. 9, no. 8, p. 1546, Apr. 2019.

[176] Z. Yuan, S. Feng, S. Chen, W. Jing, L. Zhao, and Z. Jiang, "A ferromagnetic particle sensor based on a honeycomb permanent magnet for high precision and high throughput," *IEEE Trans. Instrum. Meas.*, vol. 71, pp. 1–9, 2022.

[177] D. Murzin et al., "Ultrasensitive magnetic field sensors for biomedical applications," *Sensors*, vol. 20, no. 6, p. 1569, Mar. 2020.

[178] A. Grosz, M. J. Haji-Sheikh, and S. C. Mukhopadhyay, *High Sensitivity Magnetometers*, vol. 19, S. C. Mukhopadhyay, Ed. Palmerston North, New Zealand: School of Engineering and Advanced Technology (SEAT), Massey University, 2017.

[179] C. Min et al., "Integrated microHall magnetometer to measure the magnetic properties of nanoparticles," *Lab Chip*, vol. 17, no. 23, pp. 4000–4007, 2017.

[180] C.-C. Huang, X. Zhou, and D. A. Hall, "Giant magnetoresistive biosensors for time-domain magnetorelaxometry: A theoretical investigation and progress toward an immunoassay," *Sci. Rep.*, vol. 7, no. 1, pp. 1–10, Apr. 2017.

[181] L. Hao, D. Cox, P. See, J. Gallop, and O. Kazakova, "Magnetic nanoparticle detection using nano-SQUID sensors," *J. Phys. D, Appl. Phys.*, vol. 43, no. 47, Dec. 2010, Art. no. 474004.

[182] R. Kotitz et al., "SQUID based remanence measurements for immunoassays," *IEEE Trans. Appl. Supercond.*, vol. 7, no. 2, pp. 3678–3681, Jun. 1997.

[183] S. Tanaka, H. Ota, Y. Kondo, Y. Tamaki, S. Kobayashi, and S. Noguchi, "Detection of magnetic nanoparticles in lymph nodes of rat by high T_c SQUID," *IEEE Trans. Appl. Supercond.*, vol. 13, no. 2, pp. 377–380, Jun. 2003.

[184] K. Enpuku, K. Inoue, K. Soejima, K. Yoshinaga, H. Kuma, and N. Hamasaki, "Magnetic immunoassays utilizing magnetic markers and a high-T_c SQUID," *IEEE Trans. Appl. Supercond.*, vol. 15, no. 2, pp. 660–663, 2005.

[185] V. Nabaei, R. Chandrawati, and H. Heidari, "Magnetic biosensors: Modelling and simulation," *Biosensors Bioelectron.*, vol. 103, pp. 69–86, Apr. 2018.

[186] S.-J. Lee et al., "SQUID-based ultralow-field MRI of a hyperpolarized material using signal amplification by reversible exchange," *Sci. Rep.*, vol. 9, no. 1, pp. 1–8, Aug. 2019.

[187] H.-J. Krause et al., "Detection of magnetic contaminations in industrial products using HTS SQUIDs," *IEEE Trans. Appl. Supercond.*, vol. 15, no. 2, pp. 729–732, Jun. 2005.

[188] S. Tanaka, T. Akai, Y. Kitamura, Y. Hatsukade, T. Otani, and S. Suzuki, "Two-channel HTS SQUID gradiometer system for detection of metallic contaminants in lithium-ion battery," *IEEE Trans. Appl. Supercond.*, vol. 21, no. 3, pp. 424–427, Jun. 2011.

[189] S. Ge, X. Shi, J. R. Baker, M. M. Banaszak Holl, and B. G. Orr, "Development of a remanence measurement-based SQUID system with in-depth resolution for nanoparticle imaging," *Phys. Med. Biol.*, vol. 54, no. 10, pp. N177–N188, May 2009.

[190] T. Shijo, S. Kurachi, Y. Uchino, Y. Noda, H. Yamada, and T. Tanaka, "High-frequency induction heating for small-foreign-metal particle detection using 400 kHz SiC-MOSFETs inverter," in *Proc. IEEE Energy Convers. Congr. Expo. (ECCE)*, Oct. 2017, pp. 5133–5138.

[191] J. Lenz and A. S. Edelstein, "Magnetic sensors and their applications," *IEEE Sensors J.*, vol. 6, no. 3, pp. 631–649, Jun. 2006.

[192] G. Mihajlović et al., "Detection of single magnetic bead for biological applications using an InAs quantum-well micro-Hall sensor," *Appl. Phys. Lett.*, vol. 87, no. 11, Sep. 2005, Art. no. 112502.

[193] M. Volmer and M. Avram, "Using permalloy based planar Hall effect sensors to capture and detect superparamagnetic beads for lab on a chip applications," *J. Magn. Magn. Mater.*, vol. 381, pp. 481–487, May 2015.

[194] I. Inthawatkul, W. Sriratana, and S. Satthamsakul, "Measurement of metal particles in oil lubricant using Hall effect sensor under temperature conditions," in *Proc. 56th Annu. Conf. Soc. Instrum. Control Engineers Jpn. (SICE)*, Sep. 2017, pp. 731–735.

[195] J. Schütt et al., "Two orders of magnitude boost in the detection limit of droplet-based micro-magnetofluidics with planar Hall effect sensors," *ACS Omega*, vol. 5, no. 32, pp. 20609–20617, Aug. 2020.

[196] Y. Li et al., "Nanomagnetic competition assay for low-abundance protein biomarker quantification in unprocessed human sera," *J. Amer. Chem. Soc.*, vol. 132, no. 12, pp. 4388–4392, Mar. 2010.

[197] L. T. Hien et al., "DNA-magnetic bead detection using disposable cards and the anisotropic magnetoresistive sensor," *Adv. Natural Sci., Nanoscience Nanotechnol.*, vol. 7, no. 4, Oct. 2016, Art. no. 045006.

[198] L. K. Quynh et al., "Detection of magnetic nanoparticles using simple AMR sensors in wheatstone bridge," *J. Sci., Adv. Mater. Devices*, vol. 1, no. 1, pp. 98–102, Mar. 2016.

[199] S.-J. Han, L. Xu, R. J. Wilson, and S. X. Wang, "A novel zero-drift detection method for highly sensitive GMR biochips," *IEEE Trans. Magn.*, vol. 42, no. 10, pp. 3560–3562, Oct. 2006.

[200] A. Manteca, M. Mujika, and S. Arana, "GMR sensors: Magnetoresistive behaviour optimization for biological detection by means of superparamagnetic nanoparticles," *Biosensors Bioelectron.*, vol. 26, no. 8, pp. 3705–3709, Apr. 2011.

[201] C. Marquina et al., "GMR sensors and magnetic nanoparticles for immuno-chromatographic assays," *J. Magn. Magn. Mater.*, vol. 324, no. 21, pp. 3495–3498, Oct. 2012.

[202] H. Lei, K. Wang, X. Ji, and D. Cui, "Contactless measurement of magnetic nanoparticles on lateral flow strips using tunneling magnetoresistance (TMR) sensors in differential configuration," *Sensors*, vol. 16, no. 12, p. 2130, Dec. 2016.

[203] X.-H. Mu et al., "A new rapid detection method for ricin based on tunneling magnetoresistance biosensor," *Sens. Actuators B, Chem.*, vol. 284, pp. 638–649, Apr. 2019.

[204] E. Albisetti et al., "Photolithographic bio-patterning of magnetic sensors for biomolecular recognition," *Sens. Actuators B, Chem.*, vol. 200, pp. 39–46, Sep. 2014.

[205] P. P. Sharma et al., "Integrated platform for detecting pathogenic DNA via magnetic tunneling junction-based biosensors," *Sens. Actuators B, Chem.*, vol. 242, pp. 280–287, Apr. 2017.

[206] Z. Mao, W. Zhai, Y. Shen, S. Zhao, and J. Gao, "Advanced metal detection system based on TMR sensor array," *J. Magn. Magn. Mater.*, vol. 543, Feb. 2022, Art. no. 168601.

[207] K. R. Astley, P. Anuzis, I. C. D. Care, T. A. Moore, P. G. Morris, and P. D. Rees, "Monitoring the health of a fluid system," U.S. Patent 6 794 865, Sep. 21, 2004.

[208] B. Blasiak, F. C. J. M. van Veggel, and B. Tomanek, "Applications of nanoparticles for MRI cancer diagnosis and therapy," *J. Nanomater.*, vol. 2013, pp. 1–12, Jan. 2013.

[209] P. F. Doorn, P. A. Campbell, J. Worrall, P. D. Benya, H. A. McKellop, and H. C. Amstutz, "Metal wear particle characterization from metal on metal total hip replacements: Transmission electron microscopy study of periprosthetic tissues and isolated particles," *J. Biomed. Mater. Res.*, vol. 42, no. 1, pp. 103–111, Oct. 1998.

[210] E. M. Shapiro, S. Skrtic, K. Sharer, J. M. Hill, C. E. Dunbar, and A. P. Koretsky, "MRI detection of single particles for cellular imaging," *Proc. Nat. Acad. Sci. USA*, vol. 101, no. 30, pp. 10901–10906, Jul. 2004.

[211] T. Kanda et al., "Contribution of metals to brain MR signal intensity: Review articles," *Japanese J. Radiol.*, vol. 34, no. 4, pp. 258–266, Apr. 2016.

[212] K. M. Koch et al., "Off-resonance based assessment of metallic wear debris near total hip arthroplasty," *Magn. Reson. Med.*, vol. 79, no. 3, pp. 1628–1637, Mar. 2018.

[213] J. Zhuo and R. P. Gullapalli, "MR artifacts, safety, and quality control," *RadioGraphics*, vol. 26, no. 1, pp. 275–297, Jan. 2006.

[214] C. I. Urraca Del Junco, D. J. Shaw, M. P. Weaver, and T. Schwarz, "The value of radiographic screening for metallic particles in the equine foot and size of related artifacts on low-field MRI," *Veterinary Radiol. Ultrasound*, vol. 52, no. 6, pp. 634–639, Nov. 2011.

[215] D. Passeri et al., "Magnetic force microscopy: Quantitative issues in biomaterials," *Biomatter*, vol. 4, no. 1, Jan. 2014, Art. no. e29507.

[216] K. Krogsøe, M. Henneberg, and R. L. Eriksen, "Model of a light extinction sensor for assessing wear particle distribution in a lubricated oil system," *Sensors*, vol. 18, no. 12, p. 4091, 2018.
[217] J. Rheims, T. Wriedt, and K. Bauckhage, "Sizing of inhomogeneous particles by a differential laser Doppler anemometer," *Meas. Sci. Technol.*, vol. 10, no. 2, pp. 68–75, Feb. 1999.
[218] G. Wolf and H. W. Bergmann, "Investigations on melt atomization with gas and liquefied cryogenic gas," *Mater. Sci. Eng., A*, vol. 326, no. 1, pp. 134–143, Mar. 2002.
[219] W. Tscharnuter, "Photon correlation spectroscopy in particle sizing," in *Encyclopedia of Analytical Chemistry*. Holtsville, NY, USA: Brookhaven Instruments Corporation, 2000, pp. 5469–5485.
[220] S. Zhan et al., "A silver-specific DNA-based bio-assay for Ag (I) detection via the aggregation of unmodified gold nanoparticles in aqueous solution coupled with resonance Rayleigh scattering," *Anal. Methods*, vol. 4, no. 12, pp. 3997–4002, 2012.
[221] W. Witt, H. Geers, and L. Aberle, "Measurement of particle size and stability of nanoparticles in opaque suspensions and emulsions with photon cross correlation spectroscopy (PCCS)," Part Syst. Anal. Harrogate U.K., Fraunhofer Institut für Fertigungstechnik und AngewandteMaterialforschung (IFAM), Bremen, Germany, Tech. Rep., 2003.
[222] Y. Peng, C. Shi, Y. Zhu, M. Gu, and S. Zhuang, "Terahertz spectroscopy in biomedical field: A review on signal-to-noise ratio improvement," *PhotoniX*, vol. 1, no. 1, pp. 1–18, Dec. 2020.
[223] Y. Kitahara, C. Domier, M. Ikeda, A.-V. Pham, and N. C. Luhmann Jr., "Detection of small metal particles by a quasi-optical system at submillimeter wavelength," *Proc. SPIE*, vol. 9856, pp. 31–39, Apr. 2016.
[224] Z. Yang, Q. Wang, Z. Cao, X. Wang, and Y. Peng, "Quantitative analysis of metal particles concentration in the composites based on terahertz linear scatter method," *IEEE Trans. THz Sci. Technol.*, vol. 10, no. 5, pp. 490–494, Sep. 2020.
[225] N. Palka, A. Rybak, E. Czerwińska, and M. Florkowski, "Terahertz detection of wavelength-size metal particles in pressboard samples," *IEEE Trans. THz Sci. Technol.*, vol. 6, no. 1, pp. 99–107, Jan. 2016.
[226] Y. Yu et al., "Measuring impurity content in pipelines by positron annihilation," *Meas. Control*, vol. 54, nos. 3–4, pp. 485–493, Mar. 2021.
[227] D. Boyer, P. Tamarat, A. Maali, B. Lounis, and M. Orrit, "Photothermal imaging of nanometer-sized metal particles among scatterers," *Science*, vol. 297, no. 5584, pp. 1160–1163, Aug. 2002.
[228] S. Berciaud, L. Cognet, G. A. Blab, and B. Lounis, "Photothermal heterodyne imaging of individual nonfluorescent nanoclusters and nanocrystals," *Phys. Rev. Lett.*, vol. 93, no. 25, Dec. 2004, Art. no. 257402.
[229] P. M. R. Paulo et al., "Photothermal correlation spectroscopy of gold nanoparticles in solution," *J. Phys. Chem. C*, vol. 113, no. 27, pp. 11451–11457, Jul. 2009.
[230] S. Adhikari, P. Spaeth, A. Kar, M. D. Baaske, S. Khatua, and M. Orrit, "Photothermal microscopy: Imaging the optical absorption of single nanoparticles and single molecules," *ACS Nano*, vol. 14, no. 12, pp. 16414–16445, Dec. 2020.
[231] X. Hong, E. M. P. H. van Dijk, S. R. Hall, J. B. Götte, N. F. van Hulst, and H. Gersen, "Background-free detection of single 5 nm nanoparticles through interferometric cross-polarization microscopy," *Nano Lett.*, vol. 11, no. 2, pp. 541–547, Feb. 2011.
[232] C. Haiden, T. Wopelka, M. Jech, F. Keplinger, and M. J. Vellekoop, "A microfluidic chip and dark-field imaging system for size measurement of metal wear particles in oil," *IEEE Sensors J.*, vol. 16, no. 5, pp. 1182–1189, Mar. 2016.
[233] J. E. Tucker et al., "LaserNet fines optical oil debris monitor," in *Proc. JOAP Int. Condition Monit. Conf.*, 1998, pp. 117–124.
[234] J. Mabe, J. Zubia, and E. Gorritxategi, "Photonic low cost micro-sensor for in-line wear particle detection in flowing lube oils," *Sensors*, vol. 17, no. 3, p. 586, Mar. 2017.
[235] O. Mudanyali et al., "Compact, light-weight and cost-effective microscope based on lensless incoherent holography for telemedicine applications," *Lab Chip*, vol. 10, pp. 1417–1428, Apr. 2010.
[236] N. Niemiec, C. Dillier, D. R. Guildenbecher, E. L. Petersen, and W. D. Kulatilaka, "Simultaneous particle flow field characterization and metal speciation in the reaction zone of metalized AP/HTPB propellants," Sandia Nat. Lab. (SNL-NM), Albuquerque, NM, USA, Tech. Rep. SAND2018-4613C, 2018.
[237] Y. C. Mazumdar, J. D. Heyborne, and D. R. Guildenbecher, "Laser diagnostics for solid rocket propellants and explosives," in *Proc. IEEE Res. Appl. Photon. Defense Conf. (RAPID)*, Aug. 2019, pp. 1–4.
[238] D. Takhar, "Compressed sensing for imaging applications," Ph.D. thesis, Dept. Elect. Comput. Eng., Rice Univ., Houston, TX, USA, 2008.
[239] R. Appleby and H. B. Wallace, "Standoff detection of weapons and contraband in the 100 GHz to 1 THz region," *IEEE Trans. Antennas Propag.*, vol. 55, no. 11, pp. 2944–2956, Nov. 2007.
[240] G.-J. Kim, J.-I. Kim, S.-G. Jeon, J. Kim, K.-K. Park, and C.-H. Oh, "Enhanced continuous-wave terahertz imaging with a horn antenna for food inspection," *J. Infr., Millim., THz Waves*, vol. 33, no. 6, pp. 657–664, Jun. 2012.
[241] G. Ok, K. Park, H. S. Chun, H.-J. Chang, N. Lee, and S.-W. Choi, "High-performance sub-terahertz transmission imaging system for food inspection," *Biomed. Opt. Exp.*, vol. 6, no. 5, pp. 1929–1941, 2015.
[242] M. T. M. Khairi, S. Ibrahim, M. A. M. Yunus, and M. Faramarzi, "Noninvasive techniques for detection of foreign bodies in food: A review," *J. Food Process Eng.*, vol. 41, no. 6, p. e12808, 2018.
[243] S. Zappia, L. Crocco, and I. Catapano, *THz Imaging for Food Inspections: A Technology Review and Future Trends*. IntechOpen, 2021, doi: 10.5772/intechopen.97615.
[244] C. Jördens, F. Rutz, and M. Koch, "Quality assurance of chocolate products with terahertz imaging," in *Proc. Eur. Conf. Non-Destructive Test.*, 2006, pp. 1563–1621.
[245] J. A. Zeitler, "Pharmaceutical terahertz spectroscopy and imaging," in *Analytical Techniques in the Pharmaceutical Sciences*. New York, NY, USA: Springer, 2016, pp. 171–222.
[246] A. Y. Pawar, D. D. Sonawane, K. B. Erande, and D. V. Derle, "Terahertz technology and its applications," *Drug Invention Today*, vol. 5, no. 2, pp. 157–163, Jun. 2013.
[247] P. Dean et al., "Terahertz imaging using quantum cascade lasers—A review of systems and applications," *J. Phys. D, Appl. Phys.*, vol. 47, no. 37, 2014, Art. no. 374008.
[248] N. Rothbart, H. Richter, M. Wienold, L. Schrottke, H. T. Grahn, and H.-W. Hübers, "Fast 2-D and 3-D terahertz imaging with a quantum-cascade laser and a scanning mirror," *IEEE Trans. THz Sci. Technol.*, vol. 3, no. 5, pp. 617–624, Sep. 2013.
[249] S.-H. Cho et al., "Fast terahertz reflection tomography using block-based compressed sensing," *Opt. Exp.*, vol. 19, no. 17, pp. 16401–16409, 2011.
[250] B.-M. Hwang, S. H. Lee, W.-T. Lim, C.-B. Ahn, J.-H. Son, and H. Park, "A fast spatial-domain terahertz imaging using block-based compressed sensing," *J. Infr., Millim., THz Waves*, vol. 32, no. 11, pp. 1328–1336, Nov. 2011.
[251] K. Kim et al., "Adaptive compressed sensing for the fast terahertz reflection tomography," *IEEE J. Biomed. Health Informat.*, vol. 17, no. 4, pp. 806–812, Jul. 2013.
[252] L. Afsah-Hejri, P. Hajeb, P. Ara, and R. J. Ehsani, "A comprehensive review on food applications of terahertz spectroscopy and imaging," *Comprehensive Rev. Food Sci. Food Saf.*, vol. 18, no. 5, pp. 1563–1621, Sep. 2019.
[253] A. Ren et al., "State-of-the-art in terahertz sensing for food and water security—A comprehensive review," *Trends Food Sci. Technol.*, vol. 85, pp. 241–251, Mar. 2019.
[254] R. Díaz, L. Cervera, S. Fenollosa, C. Ávila, and J. Belenguer, "Hyperspectral system for the detection of foreign bodies in meat products," *Proc. Eng.*, vol. 25, pp. 313–316, Jan. 2011.
[255] T. Shijo, Y. Uchino, Y. Noda, H. Yamada, and T. Tanaka, "Iron loss reduction in the cores of induction heating coils for small-foreign-metal particle detector with a 400-kHz SiC-MOSFETs high-frequency inverter," in *Proc. Int. Power Electron. Conf. (IPEC-Niigata-ECCE Asia)*, May 2018, pp. 324–328.
[256] T. Shijo, S. Kurachi, Y. Noda, H. Yamada, and T. Tanaka, "A 400 kHz SiC-MOSFETs high-frequency inverter for small-foreign-metal particle detection," in *Proc. IEEE 2nd Annu. Southern Power Electron. Conf. (SPEC)*, Dec. 2016, pp. 1–5.
[257] T. Shijo, S. Kurachi, Y. Uchino, Y. Noda, H. Yamada, and T. Tanaka, "High-frequency induction heating for small-foreign-metal particles using SiC-MOSFETs inverter," in *Proc. IEEE 3rd Int. Future Energy Electron. Conf. ECCE Asia (IFEEC-ECCE Asia)*, Jun. 2017, pp. 615–620.
[258] T. Shijo, Y. Uchino, Y. Noda, H. Yamada, and T. Tanaka, "New IH coils for small-foreign-metal particle detection using 400 kHz SiC-MOSFETs inverter," in *Proc. IEEE Energy Convers. Congr. Expo. (ECCE)*, Sep. 2018, pp. 3602–3607.
[259] T. Shijo, Y. Uchino, Y. Noda, H. Yamada, and T. Tanaka, "New induction heating coils with reduced iron-loss in the cores for small-foreign-metal particle detector using an SiC-MOSFETs high-frequency inverter," *IEEJ J. Ind. Appl.*, vol. 8, no. 5, pp. 803–812, 2019.

[260] T. Akada, T. Shijo, Y. Noda, H. Yamada, and T. Tanaka, "New I-shaped core of induction heating coil for small-foreign-metal particles detector using an SiC-MOSFET high-frequency inverter," in *Proc. 21st IEEE Hiroshima Branch Student Symp.*, Okayama, Japan, 2019.

[261] T. Kanai, "Principle and use of inspection systems for food contaminants," Anritsu Tech. Rev., Tech. Rep. 22, 2014, pp. 45–54.

[262] L. Schoeman, P. Williams, A. du Plessis, and M. Manley, "X-ray microcomputed tomography (μCT) for non-destructive characterisation of food microstructure," *Trends Food Sci. Technol.*, vol. 47, pp. 10–24, Jan. 2016.

[263] K. Morita, Y. Ogawa, C. N. Thai, and F. Tanaka, "Soft X-ray image analysis to detect foreign materials in foods," *Food Sci. Technol. Res.*, vol. 9, no. 2, pp. 137–141, 2003.

[264] J.-S. Kwon, J.-M. Lee, and W.-Y. Kim, "Real-time detection of foreign objects using X-ray imaging for dry food manufacturing line," in *Proc. IEEE Int. Symp. Consum. Electron.*, Apr. 2008, pp. 1–4.

[265] H. Einarsdóttir et al., "Novelty detection of foreign objects in food using multi-modal X-ray imaging," *Food Control*, vol. 67, pp. 39–47, Sep. 2016.

[266] T. Sato and Y. Matoba, "Rapid detection and element identification of fine metal particles for underpinning battery quality," *Hitachi Rev.*, vol. 65, no. 7, p. 263, 2016.

[267] S. F. Grebe and W. Jueling, "A method for the detection of metal particles in human tissues," *Der Radiologe*, vol. 2, pp. 312–314, Aug. 1962.

[268] E.-M. Braig et al., "Simultaneous wood and metal particle detection on dark-field radiography," *Eur. Radiol. Exp.*, vol. 2, no. 1, pp. 1–7, Dec. 2018.

[269] E.-M. Braig et al., "X-ray dark-field radiography: Potential for visualization of monosodium urate deposition," *Investigative Radiol.*, vol. 55, no. 8, pp. 494–498, 2020.

[270] J. Andrejewski et al., "Whole-body X-ray dark-field radiography of a human cadaver," *Eur. Radiol. Experim.*, vol. 5, no. 1, pp. 1–9, Dec. 2021.

[271] A. Jean E. Brown and R. Mulholland, "Using microfocus X-radiography and other techniques to create a digital watermark database," *Stud. Conservation*, vol. 47, no. 3, pp. 21–26, Sep. 2002.

[272] D. H. Larsson, W. Vågberg, A. Yaroshenko, A. Ö. Yildirim, and H. M. Hertz, "High-resolution short-exposure small-animal laboratory X-ray phase-contrast tomography," *Sci. Rep.*, vol. 6, no. 1, pp. 1–8, Dec. 2016.

[273] M. Tesařová et al., "An interactive and intuitive visualisation method for X-ray computed tomography data of biological samples in 3D portable document format," *Sci. Rep.*, vol. 9, no. 1, pp. 1–8, Oct. 2019.

[274] E. Laurien, T. Stürzel, and M. Zhou, "Unsteady void measurements within debris beds using high speed X-ray tomography," *Nucl. Eng. Des.*, vol. 312, pp. 277–283, Feb. 2017.

[275] D. R. Baker et al., "An introduction to the application of X-ray microtomography to the three-dimensional study of igneous rocks," *Lithos*, vol. 148, pp. 262–276, Sep. 2012.

[276] R. P. Haff and N. Toyofuku, "X-ray detection of defects and contaminants in the food industry," *Sens. Instrum. Food Quality Saf.*, vol. 2, no. 4, pp. 262–273, Dec. 2008.

[277] I. Kryukov, S. Böhm, and M. Schach, "Shearography as non-destructive testing method in the application of adhesive tapes," in *Proc. 19th World Conf. Non-Destructive Test.*, Munich, Germany, 2016, vol. 21, no. 7. [Online]. Available: https://www.ndt.net/search/docs.php3?id=19317

[278] M. Lukas and R. J. Yurko, "Current technology in oil analysis spectrometers and what we may expect in the future," in *Proc. Joint Conf. Technol. Showcase Integr. Monit. Diagnostics Failure Prevenion*, Mobile, AL, USA. Pensacola, FL, USA: Joint Oil Analysis Program, Technical Support Center, Apr. 1996.

[279] M. P. Hernandez-Artiga, J. A. Muñoz-Leyva, and R. Cozar-Sievert, "Determination of wear-metals in used lubricating oils from marine engines by flame atomic absorption spectrometry," *Analyst*, vol. 117, no. 6, pp. 963–966, 1992.

[280] H. Kong, H.-G. Han, and O. K. Kwon, "A study on the application of spectrometric methods for the analysis of lubricant contaminants and wear debris," *J. KSTLE*, vol. 15, no. 2, pp. 131–140, 1999.

[281] M. Lukas, D. P. Anderson, and R. J. Yurko, "New development and functional enhancements in RDE used oil analysis spectrometers," in *Proc. Int. Oil Anal. Conf.*, 1999, pp. 1–7.

[282] M. Lukas and D. Anderson, "Analytical tools to detect and quantify large wear particles in used lubricating oil," Spectro, Chelmsford, MA, USA, Tech. Rep., 2003.

[283] M. Lukas and D. P. Anderson, "Rotrode filter spectroscopy, does it have a place in the commercial or military oil analysis laboratory?" Spectro Incorporated, Littleton, MA, USA, Tech. Rep.

[284] B. Leal, J. Ordieres, S. Capuz-Rizo, and P. Cifuentes, "Contaminants analysis in aircraft engine oil and its interpretation for the overhaul of the engine," in *Proc. WSEAS Int. Conf. Math. Comput. Sci. Eng.*, no. 5, 2009, pp. 1729–1738.

[285] A. Becker, S. Abanteriba, S. Dutton, D. Forrester, and G. Rowlinson, "On the impact of fine filtration on spectrometric oil analysis and inductive wear debris sensors," *Proc. Inst. Mech. Eng., J, J. Eng. Tribol.*, vol. 230, no. 1, pp. 78–85, Jan. 2016.

[286] K. J. Eisentraut, R. W. Newman, C. S. Saba, R. E. Kauffman, and W. E. Rhine, "Spectrometric oil analysis. Detecting engine failures before they occur," *Anal. Chem.*, vol. 56, no. 9, pp. 1086A–1094A, Aug. 1984.

[287] W. Rhine, C. SABA, and R. Kauffman, "Metal particle detection capabilities of rotating-disk emission spectrometers. Pt. 1," *Lubrication Eng.*, vol. 42, no. 12, pp. 755–761, 1986.

[288] T. Kuokkanen, P. Perämäki, I. Välimäki, and H. Rönkkömäki, "Determination of heavy metals in waste lubricating oils by inductively coupled Plasma–Optical emission spectrometry," *Int. J. Environ. Anal. Chem.*, vol. 81, no. 2, pp. 89–100, Oct. 2001.

[289] D. Ščekaturovienė and N. Višniakov, "Atomic emission spectrometric analysis in the assessment of wearing of vehicle engines," *Mater. Sci. (Medžiagotyra)*, vol. 10, pp. 15–17, 2004.

[290] I. Jeffery, "Refrigeration: On the cold front-the best refrigeration compressor for your winery," *Austral. New Zealand Grapegrower Winemaker*, no. 679, p. 54 and 56–57, 2020.

[291] R. D. Beaty and J. D. Kerber, *Concepts, Instrumentation and Techniques in Atomic Absorption Spectrophotometry*, 2nd ed. Norwalk, CT, USA: The Perkin-Elmer Corporation, 1978.

[292] B. M. Atta, M. Saleem, S. U. Haq, H. Ali, Z. Ali, and M. Qamar, "Determination of zinc and iron in wheat using laser-induced breakdown spectroscopy," *Laser Phys. Lett.*, vol. 15, no. 12, Dec. 2018, Art. no. 125603.

[293] V. C. Costa, F. A. C. Amorim, D. V. de Babos, and E. R. Pereira-Filho, "Direct determination of Ca, K, Mg, Na, P, S, Fe and Zn in bivalve mollusks by wavelength dispersive X-ray fluorescence (WDXRF) and laser-induced breakdown spectroscopy (LIBS)," *Food Chem.*, vol. 273, pp. 91–98, Feb. 2019.

[294] J. D. Pedarnig, S. Trautner, S. Grünberger, N. Giannakaris, S. Eschlböck-Fuchs, and J. Hofstadler, "Review of element analysis of industrial materials by in-line laser—Induced breakdown spectroscopy (LIBS)," *Appl. Sci.*, vol. 11, no. 19, p. 9274, Oct. 2021.

[295] H. Lee, H. Maeng, K. Kim, G. Kim, and K. Park, "Application of laser-induced breakdown spectroscopy for real-time detection of contamination particles during the manufacturing process," *Appl. Opt.*, vol. 57, no. 12, pp. 3288–3292, 2018.

[296] P. Fichet, P. Mauchien, J.-F. Wagner, and C. Moulin, "Quantitative elemental determination in water and oil by laser induced breakdown spectroscopy," *Anal. Chim. Acta*, vol. 429, no. 2, pp. 269–278, Feb. 2001.

[297] Z. Ye et al., "Copper particle contamination detection of oil-immersed transformer using laser-induced breakdown spectroscopy," *Spectrochimica Acta B, At. Spectrosc.*, vol. 167, May 2020, Art. no. 105820.

[298] D. C. S. Beddows, O. Samek, M. Liška, and H. H. Telle, "Single-pulse laser-induced breakdown spectroscopy of samples submerged in water using a single-fibre light delivery system," *Spectrochimica Acta B, At. Spectrosc.*, vol. 57, no. 9, pp. 1461–1471, Sep. 2002.

[299] M. A. Gondal, T. Hussain, and Z. H. Yamani, "Optimization of the LIBS parameters for detection of trace metals in petroleum products," *Energy Sources, A, Recovery, Utilization, Environ. Effects*, vol. 30, no. 5, pp. 441–451, Jan. 2008.

[300] A. H. Farhadian, M. K. Tehrani, M. H. Keshavarz, M. Karimi, and S. M. R. Darbani, "Relationship between the results of laser-induced breakdown spectroscopy and dynamical mechanical analysis in composite solid propellants during their aging," *Appl. Opt.*, vol. 55, no. 16, pp. 4362–4369, 2016.

[301] W. Kulatilaka and E. Petersen, "Novel laser diagnostic approaches for evaluating emissions from metal-based energetic formulations," Texas A and M Eng. Exp. Station (TEES), College Station, TX, USA, Tech. Rep. WP-2160, 2018.

[302] M. O'Neil, N. A. Niemiec, A. R. Demko, E. L. Petersen, and W. D. Kulatilaka, "Laser-induced-breakdown-spectroscopy-based detection of metal particles released into the air during combustion of solid propellants," *Appl. Opt.*, vol. 57, no. 8, pp. 1910–1917, 2018.

[303] M. O'Neil, N. Niemiec, A. Demko, E. Petersen, and W. Kulatilaka, "Ultrashort-pulse LIBS for detecting airborne metal particles from energetic material reactions," in *Proc. CLEO, Sci. Innov.*, 2018, Paper STu3N–3.

[304] X. Zhang, F. Zhang, H.-T. Kung, P. Shi, A. Yushanjiang, and S. Zhu, "Estimation of the Fe and Cu contents of the surface water in the Ebinur Lake basin based on LIBS and a machine learning algorithm," *Int. J. Environ. Res. Public Health*, vol. 15, no. 11, p. 2390, Oct. 2018.

[305] A. O. Shoyinka, "Ultra-high-speed laser-induced breakdown spectroscopy (LIBS) applications using a pulse-burst laser system," Ph.D. thesis, Dept. Mech. Eng., Texas A&M Univ., College Station, TX, USA, 2019.

[306] S. Yao, L. Zhang, Y. Zhu, J. Wu, Z. Lu, and J. Lu, "Evaluation of heavy metal element detection in municipal solid waste incineration fly ash based on LIBS sensor," *Waste Manage.*, vol. 102, pp. 492–498, Feb. 2020.

[307] Y. He et al., "Dynamic zinc and potassium release from a burning hyperaccumulator pellet and their interactions with inhibitive additives," *Fuel*, vol. 286, Feb. 2021, Art. no. 119365.

[308] F. Wang, S. Zhang, X. Yu, X. Lin, J. Li, and Y. Liu, "Quantitative measurement of the mixture ratio for ADN-based liquid propellants using laser-induced breakdown spectroscopy," *J. Anal. At. Spectrometry*, vol. 36, no. 9, pp. 1996–2006, 2021.

[309] M. Burnette, S. D. Chambreau, and G. L. Vaghjiani, "Iridium catalyst detection by laser induced breakdown spectroscopy," *Spectrochimica Acta B, At. Spectrosc.*, vol. 187, Jan. 2022, Art. no. 106327.

[310] R. N. Zare, "My life with LIF: A personal account of developing laser-induced fluorescence," *Annu. Rev. Anal. Chem.*, vol. 5, no. 1, pp. 1–14, Jul. 2012.

[311] E. A. Lymer, M. G. Daly, K. T. Tait, V. E. Di Cecco, and E. A. Lalla, "UV laser-induced fluorescence spectroscopy as a non-destructive technique for mineral and organic detection in carbonaceous chondrites," *Meteoritics Planet. Sci.*, vol. 55, no. 10, pp. 2287–2300, Oct. 2020.

[312] N. Britun and J. Hnilica, "Optical spectroscopy for sputtering process characterization," *J. Appl. Phys.*, vol. 127, no. 21, Jun. 2020, Art. no. 211101.

[313] J. P. Crimaldi, "Planar laser induced fluorescence in aqueous flows," *Exp. Fluids*, vol. 44, no. 6, pp. 851–863, Jun. 2008.

[314] G. Vilmart et al., "Detection of iron atoms by emission spectroscopy and laser-induced fluorescence in solid propellant flames," *Appl. Opt.*, vol. 57, no. 14, pp. 3817–3828, 2018.

[315] G. Vilmart, N. Dorval, R. Devillers, Y. Fabignon, B. Attal-Trétout, and A. Bresson, "Imaging aluminum particles in solid-propellant flames using 5 kHz LIF of al atoms," *Materials*, vol. 12, no. 15, p. 2421, Jul. 2019.

[316] I. Nelson, "Compact X-ray fluorescence spectrometer for real-time wear metal analysis of lubrucating oils," U.S. Patent 5 982 847, Nov. 9, 1999.

[317] W. E. Maddox and W. G. Kelliher, "X-ray fluorescence analysis of wear metals in used lubricating oils," *Adv. X-Ray Anal.*, vol. 29, pp. 497–502, Mar. 1985.

[318] Z. Yang, X. Hou, and B. T. Jones, "Determination of wear metals in engine oil by mild acid digestion and energy dispersive X-ray fluorescence spectrometry using solid phase extraction disks," *Talanta*, vol. 59, no. 4, pp. 673–680, Mar. 2003.

[319] G. Cumming and I. G. McDonald, "The determination of iron in lubricating oils by X-ray fluorescence spectrometry," *Wear*, vol. 103, no. 1, pp. 57–66, May 1985.

[320] K. Pollmann, M. Merroun, J. Raff, C. Hennig, and S. Selenska-Pobell, "Manufacturing and characterization of pd nanoparticles formed on immobilized bacterial cells," *Lett. Appl. Microbiol.*, vol. 43, no. 1, pp. 39–45, Jul. 2006.

[321] N. J. Creamer et al., "Novel supported pd hydrogenation bionanocatalyst for hybrid homogeneous/heterogeneous catalysis," *Catal. Today*, vol. 128, nos. 1–2, pp. 80–87, Oct. 2007.

[322] F. Vallejos-Burgos et al., "Pyrolyzed phthalocyanines as surrogate carbon catalysts: Initial insights into oxygen-transfer mechanisms," *Fuel*, vol. 99, pp. 106–117, Sep. 2012.

[323] L. Guczi et al., "AuPd bimetallic nanoparticles on TiO_2: XRD, TEM, in situ EXAFS studies and catalytic activity in CO oxidation," *J. Mol. Catal. A, Chem.*, vols. 204–205, pp. 545–552, Sep. 2003.

[324] K. O'Connell and J. R. Regalbuto, "High sensitivity silicon slit detectors for 1 nm powder XRD size detection limit," *Catal. Lett.*, vol. 145, no. 3, pp. 777–783, Mar. 2015.

[325] C.-K. Chang, Y.-J. Chen, and C.-T. Yeh, "Characterizations of alumina-supported gold with temperature-programmed reduction," *Appl. Catal. A, Gen.*, vol. 174, nos. 1–2, pp. 13–23, Nov. 1998.

[326] S. J. Parikh, K. W. Goyne, A. J. Margenot, F. N. Mukome, and F. J. Calderón, "Soil chemical insights provided through vibrational spectroscopy," *Adv. Agronomy*, vol. 126, pp. 1–148, Jan. 2014.

[327] M. Jackson and H. H. Mantsch, "Infrared spectroscopy, ex vivo tissue analysis by," in *Encyclopedia of Analytical Chemistry: Applications, Theory, and Instrumentation*. North Andover, MA, USA: Elsevier, 2006.

[328] Y. Soma-Noto and W. Sachtler, "Infrared spectra of carbon monoxide adsorbed on supported palladium and palladium-silver alloys," *J. Catal.*, vol. 32, no. 2, pp. 315–324, Feb. 1974.

[329] A. K. Datye, "Bimetallic ruthenium-gold catalysts: Characterization and catalytic behavior (electron microscopy, heterogeneous catalysts, metal-metal interactions)," Ph.D. thesis, Univ. Microfilms Int., Ann Harbor, MI, USA, 1984.

[330] K. Usman, M. A. Al-Ghouti, and M. H. Abu-Dieyeh, "The assessment of cadmium, chromium, copper, and nickel tolerance and bioaccumulation by shrub plant tetraena qataranse," *Sci. Rep.*, vol. 9, no. 1, pp. 1–11, Apr. 2019.

[331] A. Sivaramakrishna, H. S. Clayton, B. C. E. Makhubela, and J. R. Moss, "Platinum based mixed-metal clusters $(Pt_nM_m(CO)_xL_y$, M = Ru or Os; n + m = 2 to 10 and L_y = other ligands)—Synthesis, structure, reactivity and applications," *Coordination Chem. Rev.*, vol. 252, nos. 12–14, pp. 1460–1485, Jul. 2008.

[332] A. Hugon, L. Delannoy, J.-M. Krafft, and C. Louis, "Selective hydrogenation of 1, 3-butadiene in the presence of an excess of alkenes over supported bimetallic gold-palladium catalysts," *J. Phys. Chem. C*, vol. 114, no. 24, pp. 10823–10835, Jun. 2010.

[333] Y. Du, R. Liu, B. Liu, S. Wang, M.-Y. Han, and Z. Zhang, "Surface-enhanced Raman scattering chip for femtomolar detection of mercuric ion (II) by ligand exchange," *Anal. Chem.*, vol. 85, no. 6, pp. 3160–3165, Mar. 2013.

[334] P. Ndokoye, J. Ke, J. Liu, Q. Zhao, and X. Li, "L-cysteine-modified gold nanostars for SERS-based copper ions detection in aqueous media," *Langmuir*, vol. 30, no. 44, pp. 13491–13497, Nov. 2014.

[335] R. L. Wright and P. W. Centers, *Effect of Sample Volume on Quantitation of Ferrographic Data*. Wright-Patterson Air Force Base, OH, USA: Aero Propulsion Laboratory, Air Force Wright Aeronautical Laboratories, 1988.

[336] R. L. Wright and P. W. Centers, "An improved method of ferrographic quantitation," *Wear*, vol. 129, no. 2, pp. 285–292, Feb. 1989.

[337] W.-F. Kuo, Y.-C. Chiou, and R.-T. Lee, "Fundamental characteristics of wear particle deposition measurement by an improved on-line ferrographic analyzer," *Wear*, vol. 208, nos. 1–2, pp. 42–49, Jul. 1997.

[338] N. K. Myshkin, L. V. Markova, M. S. Semenyuk, H. Kong, H.-G. Han, and E.-S. Yoon, "Wear monitoring based on the analysis of lubricant contamination by optical ferroanalyzer," *Wear*, vol. 255, nos. 7–12, pp. 1270–1275, Aug. 2003.

[339] T. H. Wu, J. H. Mao, J. T. Wang, J. Y. Wu, and Y. B. Xie, "A new on-line visual ferrograph," *Tribol. Trans.*, vol. 52, no. 5, pp. 623–631, Sep. 2009.

[340] B. Li, Y. Xi, S. Feng, J. Mao, and Y.-B. Xie, "A direct reflection OLVF debris detector based on dark-field imaging," *Meas. Sci. Technol.*, vol. 29, no. 6, Jun. 2018, Art. no. 065104.

[341] F. Fajardie, J.-F. Tempere, J.-M. Manoli, O. Touret, and G. Djéga-Mariadassou, "Thermal stability of (0.15–0.35 wt%) rhodium on low-loaded ceria-supported rhodium catalysts," *Catal. Lett.*, vol. 54, no. 4, pp. 187–193, 1998.

[342] M. Gollasch, "Synthesis and characterisation of iron/cobalt bimetallic Me-NC catalysts for electrochemical oxygen reduction," Ph.D. thesis, Inst. Chem., Univ. Oldenburg, Oldenburg, Germany, 2020.

[343] A. González-Fernández, Á. Berenguer-Murcia, D. Cazorla-Amorós, and F. Cárdenas-Lizana, "Zn-promoted selective gas-phase hydrogenation of tertiary and secondary C4 alkynols over supported Pd," *ACS Appl. Mater. Interfaces*, vol. 12, no. 25, pp. 28158–28168, Jun. 2020.

[344] G. Del Angel, S. Alerasool, J. M. Domínguez, R. D. Gonzalez, and R. Gómez, "Chemical analysis of small supported Pt Ru bimetallic clusters by EDS," *Surf. Sci.*, vol. 224, nos. 1–3, pp. 407–424, Dec. 1989.

[345] N. W. Farrant and T. Luckhurst, "Effective condition monitoring of aero-engine systems using automated SEM/EDX and new diagnostic routines," in *Proc. Int. Conf. JOAP Technol. Showcase*, Mobile, AL, USA. Bristol, U.K.: Rolls-Royce Ltd., 1998, pp. 276–289.

[346] G. A. Lundeen, K. G. Shea, C. Sanderson, K. N. Bachus, and R. D. Bloebaum, "Technique for identification of submicron metal particulate from implants in histological specimens," *J. Biomed. Mater. Res.*, vol. 43, no. 2, pp. 168–174, 1998.

[347] F. Cárdenas-Lizana, Z. M. de Pedro, S. Gómez-Quero, and M. A. Keane, "Gas phase hydrogenation of nitroarenes: A comparison of the catalytic action of titania supported gold and silver," *J. Mol. Catal. A, Chem.*, vol. 326, nos. 1–2, pp. 48–54, Jul. 2010.

[348] J. Dvořáčková, H. Bielniková, and J. Mačák, "Nanopathology as a new scientific discipline. Minireview," *Ceskoslovenska Patologie*, vol. 49, no. 1, pp. 46–50, 2013.

[349] R. Moser, F. Zaccarini, W. Moser, R. Schrittwieser, and R. Kerbl, "Metals in human gall, bladder, and kidney stones based on an electron microprobe investigation," *Microsc. Microanal.*, vol. 21, no. 5, pp. 1167–1172, Oct. 2015.

[350] M. El Himer, "Innovation in condition monitoring and predictive maintenance solutions in industrial contexts," M.S. thesis, Dept. Mech. Struct. Eng. Mater. Sci., Univ. Stavanger, Stavanger, Norway, 2019.

[351] M. Kumar, D. D. Snow, Y. Li, and P. J. Shea, "Perchlorate behavior in the context of black carbon and metal cogeneration following fireworks emission at Oak Lake, Lincoln, Nebraska, USA," *Environ. Pollut.*, vol. 253, pp. 930–938, Oct. 2019.

[352] V. Neimash et al., "Formation of silver nanoparticles in PVA-PEG hydrogel under electron irradiation," *Ukrainian J. Phys.*, vol. 64, no. 1, p. 41, 2019.

[353] G. Gentile et al., "A brief review of scanning electron microscopy with energy-dispersive X-ray use in forensic medicine," *Amer. J. Forensic Med. Pathol.*, vol. 41, no. 4, pp. 280–286, 2020.

[354] A. Gonzalez-Fernandez, "Gas phase catalytic hydrogenation of alkynols over palladium and nickel catalysts," Ph.D. thesis, School Eng. Phys. Sci., Heriot-Watt Univ., Edinburgh, U.K., 2020.

[355] W. Habicht, S. Behrens, N. Boukis, and E. Dinjus, "Scanning transmission type imaging and analysis (EDX) of protein supported metallic nanoparticles," *GIT Imag. Microsc.*, vol. 1, pp. 42–44, Jan. 2001.

[356] D. Stokes, *Principles and Practice of Variable Pressure/Environmental Scanning Electron Microscopy (VP-ESEM)*. Hoboken, NJ, USA: Wiley, 2008.

Jack B. Jedlicki is currently pursuing the double major bachelor's degree in mathematics and physics with the University of Barcelona, Barcelona, Spain.

Since 2021, he has been conducting research at the Auto-ID Labs, Massachusetts Institute of Technology, Cambridge, MA, USA, on metal detection. He is also currently working with the Computational Precision Health (CPH) Program at the University of California at Berkeley (UC Berkeley), Berkeley, CA, USA, and the University of California at San Francisco (UCSF), San Francisco, CA, USA. He is interested in researching the use of physics, mathematics, and artificial intelligence (AI) for solving healthcare-related problems.

Denise Tellbach received the bachelor's degree from RWTH Aachen University, Aachen, Germany, in 2016, and the double master's degree in management science and mechanical engineering from RWTH Aachen University and Tsinghua University, Beijing, China, in 2018. She is currently pursuing the bachelor's degree in mechanical engineering with the Auto-ID Labs, Massachusetts Institute of Technology, Cambridge, MA, USA.

She is working, as a part of her doctoral dissertation, on integrating artificial intelligence (AI) with multimodal sensing at the Auto-ID Labs. She is interested in vision- and radio frequency-based sensor technologies for material and defect detection in vaccine production, recycling, and picking tasks.

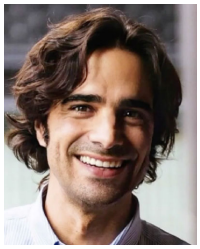

Brian Subirana received the M.B.A. degree from the MIT Sloan School of Management, Cambridge, MA, USA, and the Ph.D. degree in artificial intelligence (AI) from the Computer Science & Artificial Intelligence Laboratory (CSAIL), Massachusetts Institute of Technology (MIT), Cambridge.

He is on the faculty at the Massachusetts Institute of Technology and at Harvard University, Cambridge, MA, USA, and Full Professor of Artificial Intelligence at EADA Business School, Barcelona, Spain. He has been affiliated with MIT for over two decades, including being Director of the MIT Auto-ID Lab where the research reported here was conducted. His research centers at the crossroads of the Internet of Things (IoT) and artificial intelligence (AI).